Title

Evasion of Superinfection Exclusion and Elimination of Primary Viral RNA by an Adapted Strain of Hepatitis C Virus

Journal

Journal of Virology, 87(24)

ISSN

0022-538X

Authors

Webster, Brian
Ott, Melanie
Greene, Warner C

Publication Date

2013-12-15

DOI

10.1128/jvi.02465-13

Peer reviewed

JVI Journals.ASM.org

Evasion of Superinfection Exclusion and Elimination of Primary Viral RNA by an Adapted Strain of Hepatitis C Virus

Brian Webster,[a,b] Melanie Ott,[a,c] Warner C. Greene[a,c,d]

Gladstone Institute of Virology and Immunology,[a] Biomedical Sciences Graduate Program,[b] and Departments of Medicine[c] and Microbiology and Immunology,[d] University of California, San Francisco, San Francisco, California, USA

Cells that are productively infected by hepatitis C virus (HCV) are refractory to a second infection by HCV via a block in viral replication known as superinfection exclusion. The block occurs at a postentry step and likely involves translation or replication of the secondary viral RNA, but the mechanism is largely unknown. To characterize HCV superinfection exclusion, we selected for an HCV variant that could overcome the block. We produced a high-titer HC-J6/JFH1 (Jc1) viral genome with a fluorescent reporter inserted between NS5A and NS5B and used it to infect Huh7.5 cells containing a Jc1 replicon. With multiple passages of these infected cells, we isolated an HCV variant that can superinfect cells at high levels. Notably, the superinfectious virus rapidly cleared the primary replicon from superinfected cells. Viral competition experiments, using a novel strategy of sequence-barcoding viral strains, as well as superinfection of replicon cells demonstrated that mutations in E1, p7, NS5A, and the poly(U/UC) tract of the 3′ untranslated region were important for superinfection. Furthermore, these mutations dramatically increased the infectivity of the virus in naive cells. Interestingly, viruses with a shorter poly(U/UC) and an NS5A domain II mutation were most effective in overcoming the postentry block. Neither of these changes affected viral RNA translation, indicating that the major barrier to postentry exclusion occurs at viral RNA replication. The evolution of the ability to superinfect after less than a month in culture and the concomitant exclusion of the primary replicon suggest that superinfection exclusion dramatically affects viral fitness and dynamics *in vivo*.

In superinfection exclusion, a cell productively infected with a specific virus becomes resistant to infection with a homologous virus. This process has been described for several viruses, including human immunodeficiency virus (HIV) (1), Sindbis virus (2), duck hepatitis B virus (3), and citrus tristeza virus (4), in a broad range of hosts. Cells infected with or actively replicating hepatitis C virus (HCV) also become refractory to further HCV infection (5, 6). The superinfection block occurs at the level of translation or replication of the incoming secondary viral RNA (5–7), which is similar to the case of the related pestivirus bovine diarrhea virus (8). The exact mechanism is unclear. Since HCV RNA levels quickly plateau in infected cells *in vitro*, a superinfection block at the level of RNA translation or replication suggests that access to the necessary host factor(s) is rate limiting. This has clear implications for HCV treatment. By definition, a rate-limiting host factor is critical for the replication of the virus and may be a unique target in future therapies.

Superinfection exclusion itself also has clear implications for treating HCV infection. Since viral recombination requires a host cell to be productively replicating two genomes, superinfection exclusion would be expected to effectively prevent viral recombination. If, however, HCV could successfully superinfect cells, the evolution of drug and/or vaccine resistance and transfer of these characteristics between strains would be greatly enhanced. Viral variants capable of superinfection could result in an even greater degree of immune escape variants and drug-resistant strains within this already variable virus.

In the present study, we sought to determine how various viral and host factors relate to the exclusion process and whether HCV can overcome superinfection exclusion. To do this, we used a modified variant of an HCV fluorescent reporter viral genome based on the highly infectious HC/J6-JFH1 (Jc1) chimera (9). These reporter genomes have a fluorescent protein inserted between NS5A and NS5B and are significantly more infectious than standard HCV reporter strains (10–12). With this fluorescent reporter, we unambiguously distinguished multiple infections within one cell. We used these highly infectious reporter genomes to select for an HCV that could superinfect cells with high efficiency. By sequence analysis and characterization of the mutations in the superinfecting strain, we found that a mutation in domain II of NS5A and a deletion in the poly(U/UC) region of the 3′ untranslated region (3′UTR) are critical for HCV to overcome postentry superinfection exclusion. We further showed that the ability to superinfect is partially restricted by the HCV genotype of the cells and that this ability generally increases the infectivity of the virus *in vitro*.

MATERIALS AND METHODS

Cells and culture conditions. Huh7.5 cells, kindly provided by C. M. Rice (Rockefeller University) (13), were maintained in Dulbecco modified Eagle medium (DMEM), supplemented with 10% fetal bovine serum, 2 mM L-glutamine, 100 IU of penicillin/ml, and 100 μg of streptomycin/ml (Mediatech). Cells were passaged every 3 days or when they became confluent. For isolation of replicon cell lines, cells were selected with blasticidin (10 μg/ml; Invitrogen) or G418 sulfate (1 mg/ml; Axenia Biologics) at 2 to 3 days posttransfection. Cell lines transfected with the Con1 SGR/$^{NS5A\text{-}GFP}$ replicon were further enriched for the presence of the

Received 26 August 2013 Accepted 25 September 2013
Published ahead of print 2 October 2013
Address correspondence to Warner C. Greene, wgreene@gladstone.ucsf.edu.
Supplemental material for this article may be found at http://dx.doi.org/10.1128/JVI.02465-13.

doi:10.1128/JVI.02465-13

replicon by fluorescent-activated cell sorting (FACS) after a period of at least 21 days of selection (FACS Aria III; BD Biosciences). Monoclonal replicon cell lines were obtained by limiting dilution of transfected cells. To obtain replicon-cured cell lines, the monoclonal Jc1/ΔE1E2$^{NS5A\text{-}GFP\text{-}Bsd}$ replicon cell line was treated with 100 U of recombinant human alpha interferon (IFN-α; R&D Systems)/ml for 2 weeks, followed by a recovery period of at least 9 days without IFN-α treatment.

Plasmid construction. The production of the various plasmids and other DNA fragments used in the study are described in detail in the supplementary material.

Production of Huh7.5 cell lines by lentiviral transduction. Lentiviral particles were produced using an HIV-1-based vesicular stomatitis virus G-pseudotyped lentiviral system, as described (14). Jc1/ΔE1E2$^{NS5A\text{-}FLuc\text{-}BSD}$ replicon cells were transduced with *Renilla* luciferase-encoding lentiviruses (pSicoR RLuc). The resulting cell line was termed 7.5-RLuc Jc1/ΔE1E2$^{NS5A\text{-}FLuc\text{-}BSD}$.

RNA synthesis and transfection. *In vitro* transcription of viral RNA and electroporation was carried out as described (15, 16), with minor modifications. Viral RNA or firefly luciferase construct RNA was transcribed using a Megascript T7 kit (Ambion), and capped *Renilla* luciferase RNA was transcribed using the mMessage T7 kit (Ambion). All transcripts were purified by lithium chloride precipitation. For production of virus or supertransfection experiments, 7.5×10^6 Huh7.5 or Jc1/ΔE1E2$^{NS5A\text{-}GFP\text{-}Bsd}$ replicon cells were electroporated with a total of 10 μg of viral RNA. In experiments using luciferase constructs to assess viral translation, 5.63×10^6 Huh7.5 cells were transfected with 5 μg of the firefly luciferase reporter or 10 μg of the various Jc1/$^{NS5AB\text{-}FLuc}$-GND RNAs, mixed with 1 μg of capped *Renilla* luciferase RNA. In some cases, poly(A) carrier RNA (Qiagen) was used as a transfection control.

Virus production, titration, and infections. For virus production, 1 to 5 days after initial transfection, supernatants were collected from cultures. During serial passage of the superinfecting virus over Jc1/ΔE1E2$^{NS5A\text{-}GFP\text{-}Bsd}$ replicon cells, viral supernatants were collected from 3 to 12 days postinfection. The viral supernatants were clarified by filtration (0.2-μm pore size; Steriflip; Millipore) and stored at −80°C. HCV virions in the supernatants were titrated by HCV core antigen enzyme-linked immunosorbent assay (ELISA), subjected to reverse transcriptase PCR (RT-PCR), or assessed for viral focus-forming units (FFU).

The HCV core antigen ELISA (CellBiolabs) was carried out according to the manufacturer's protocol with a 1:2 dilution of viral supernatant in Dulbecco phosphate-buffered saline without Ca^{2+} or Mg^{2+} (DPBS; Mediatech). For RT-PCR analysis, viral RNA was purified from 200 μl of viral supernatants by TRIzol extraction (Invitrogen). Reverse transcription and subsequent quantitative PCR was performed in one step with the Quantitect probe RT-PCR system (Qiagen). Quantitative PCR was performed on a 7900HT fast real-time PCR system (Applied Biosystems). A probe-primer set corresponding to the HCV core region was used (17).

Viral FFU were assessed by infecting naive Huh7.5 cells with various dilutions of viral supernatants, followed by detection of infected cells by flow cytometry 3 days later, as described (18). HCV-infected cells were identified by the presence of the virally derived fluorescent reporter or immunostaining for double-stranded RNA (dsRNA). Viral FFU calculations were based on counts of 1 to 10% fluorescent protein-positive or dsRNA-positive cells. Flow cytometry-based counts of viral FFU were in close agreement to the standard limiting dilution method (19) of assessing FFU titers (data not shown).

After normalizing to HCV core/ml, HCV genome equivalents/ml, or FFU/ml, naive or replicon cell lines were infected with clarified supernatants overnight. The exception was during serial passage of the superinfecting virus over Jc1/ΔE1E2$^{NS5A\text{-}GFP\text{-}Bsd}$ replicon cells; in this case, the virus was not normalized before infection. Infected cells were passaged approximately every 3 days. When infecting replicon cell lines, antibiotics (G418 or blasticidin) were removed at the time of infection for the duration of the culture.

Magnetic bead transfection and cell isolation. A mixture of a total of 7.5×10^6 Jc1/ΔE1E2$^{NS5A\text{-}GFP\text{-}Bsd}$ polyclonal replicon cells and 7.5-H2B-EFBP2 cells (17) was transfected with 10 μg of Jc1/$^{NS5AB\text{-}mKO2\text{-}Bsd}$ RNA. Three days later, the cells were transfected with 10 pg of iron/cell of FeOLabel-Texas Red paramagnetic beads in serum-free DMEM, according to the manufacturer's protocol (Bulldog Bio). After transfection, FeOLabel-positive cells were isolated by magnetic separation on an LS magnetic column (Miltenyi). The FeOLabel-positive cells were immediately mixed with 3.75×10^6 infection-naive Jc1/ΔE1E2$^{NS5A\text{-}GFP\text{-}Bsd}$ polyclonal replicon cells and 3.75×10^6 7.5-H2B-EFBP2 cells. Three days later, the FeOLabel-negative cells were isolated by negative selection of the entire mixture of cells on an LS magnetic column.

Sequencing of viral RNA and viral barcode analysis. Supernatants were collected from infected or viral RNA-transfected cells and clarified by filtration at 0.2 μm. The supernatants were concentrated by ultrafiltration in 100-kDa MWCO Amicon-15 or Centricon columns (Millipore). A total of 30 μg of poly(A) carrier RNA (Qiagen) was added, and viral RNA was isolated from the concentrated supernatant by TRIzol extraction (Invitrogen), followed by LiCl precipitation (Ambion) to further purify the RNA.

For direct viral RNA sequencing, cDNA was prepared by random hexamer-mediated reverse transcription with a Superscript III first-strand synthesis kit (Invitrogen). PCR was carried out on eight overlapping regions of the Jc1/$^{NS5AB\text{-}mKO2\text{-}Bsd}$ genome with the primers in Table S1 in the supplemental material. The resulting PCR products were cloned into pCR4 Topo (Invitrogen), and the resulting clones were sequenced. Alignment and sequence analysis were performed with the Sequencher 4.9 program (Gene Codes).

For viral barcode analysis from Jc1/$^{NS5AB\text{-}Barcode}$-transfected or -infected cells, cDNA was prepared and amplified by gene-specific primer-mediated reverse transcription with a Superscript III one-step RT-PCR kit (Invitrogen), using the primers NS5ABmcs1 and Jc1_Amplicon_15R (see Table S2 in the supplemental material). To generate barcode concatemers, cDNA amplicons were subjected to a second nested fusion PCR using primers Barcode_LIC_Fw_5 and Barcode_LIC_Rev_5 (74-nucleotide [nt] amplicon) or Barcode_LIC_Fw_3 and Barcode_LIC_Rev_3 (86-nt amplicon). Overlap extension by the polymerase caused long barcode concatemers to form during PCR due to complementary regions in the 5′ portion of both primers. Concatemeric products containing multiple barcodes (750 to 2,000 bp long) were gel purified and cloned into pCR Blunt II Topo. Inserts were amplified by colony PCR using the primers M13 Forward (−20) and M13 Reverse; the PCR products were cleaned up using Exonuclease I and FastAP alkaline phosphatase (Fermentas) and sequenced using the M13 Reverse primer.

Flow cytometry. Cells to be analyzed by flow cytometry were trypsinized and treated for at least 1 h in 4% paraformaldehyde. For analysis of dsRNA, the cells were permeabilized in 90% methanol–10% DPBS for 1 h at −20°C. The cells were stained with anti-dsRNA antibody (J2; English and Scientific Consulting), followed by staining with a polyclonal anti-mouse immunoglobulin allophycocyanin antibody (BD Biosciences). The cells were analyzed for fluorescence on an LSRII flow cytometer equipped with a high-throughput microplate reader (BD Biosciences).

Luciferase assays. For viral translation studies, after electroporation cells were plated at 235×10^3 cells/well on a 12-well plate. For superinfection studies of 7.5-RLuc Jc1/ΔE1E2$^{NS5A\text{-}FLuc\text{-}BSD}$ cells, 37.5×10^3 cells/well were plated on 24-well plates. At 4 h after electroporation, or at 6 days postinfection, the cells were washed with DPBS and stored at −80°C. Firefly and *Renilla* luciferase luminescence was assessed according to the manufacturer's protocol (Dual Luciferase Assay; Promega).

Statistical analysis. Statistical analysis was carried out using Prism 5 software (GraphPad). For Fig. 5B, linear regression and analysis of covariance was used to determine whether the slopes of the exclusion curves were significantly different. For all other tests, one-way analysis of variance (ANOVA) with a Bonferroni multiple-comparison correction was used.

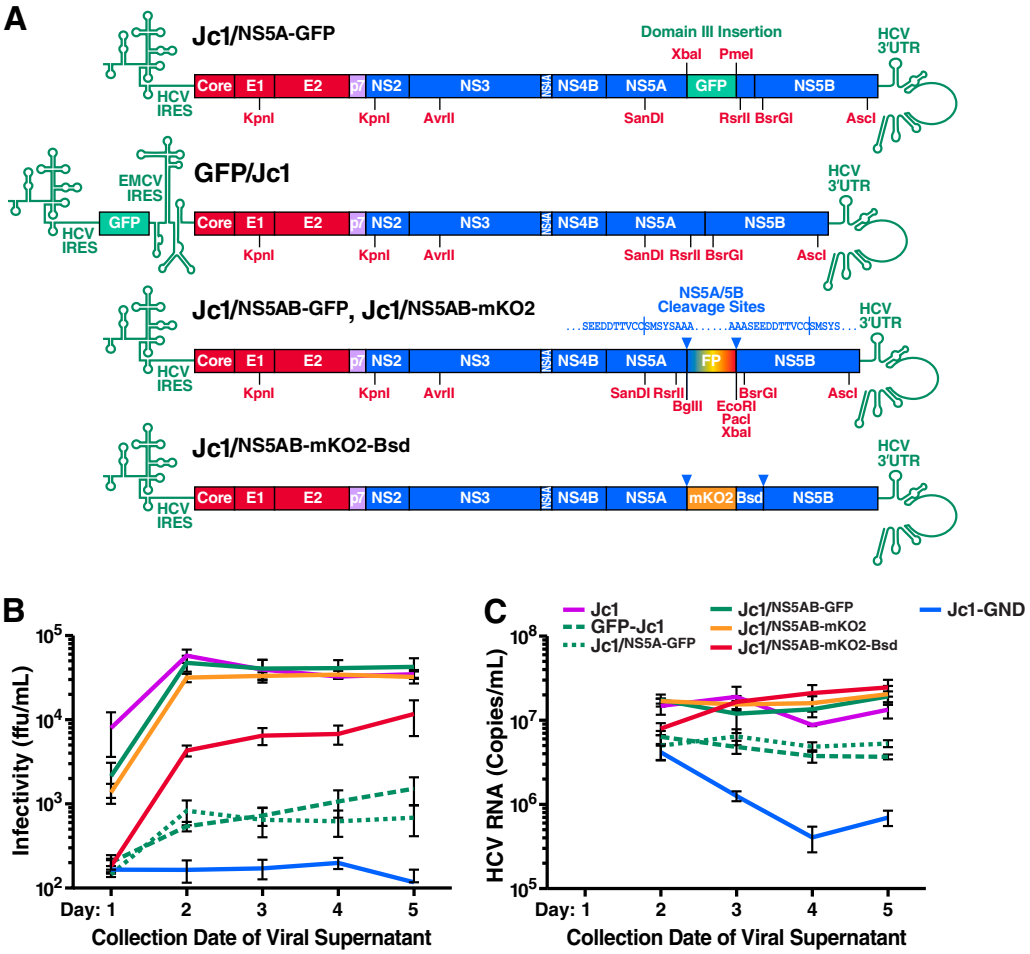

FIG 1 Construction of highly infectious reporter HCV strains. (A) Schematic diagram of HCV reporter strains. FP represents the fluorophore tag (GFP or mKO2) and Bsd represents the blasticidin resistance gene. (B and C) Huh7.5 cells were transfected with RNA transcripts of the given strains, including untagged Jc1. Supernatants were collected from days 1 to 5 after transfection and clarified by filtration. The nonreplicating Jc1-GND (polymerase defective, NS5B GDD→GND mutation) was used as a transfection control. (B) Titers of infectious HCV particles after transfection. Virus titers were obtained by limiting dilution assay. Note the higher infectious titers in the Jc1/^{NS5AB} reporter strains relative to previously described reporter strains. (C) Release of HCV RNA after transfection. RNA was isolated from supernatants after transfection and HCV RNA was quantified by real-time RT-PCR. Note the higher viral RNA levels in the Jc1/^{NS5AB} reporter strains relative to previously described reporter strains. $n = 3$ independent viral preparations and quantifications; error bars indicate the standard errors of the mean (SEM).

RESULTS

Viral genomes with reporter proteins between NS5A and NS5B are highly infectious. A successful model to study HCV superinfection exclusion and viral mutations necessary to overcome the block requires that we (i) use a highly infectious strain in the selection process and (ii) can to easily distinguish superinfected from nonsuperinfected cells in infected cultures. Although the Jc1 chimera is highly infectious, without a fluorescent reporter, the study of superinfection is difficult. Most of the existing non-culture-adapted Jc1 reporter strains were not sufficiently infectious for our purposes. The first HCV reporter strains were bicistronic viruses using a separate internal ribosome entry site (IRES) to translate the reporter protein. These viruses display a defect in replication kinetics relative to wild-type (WT) HCV (5, 20) (Fig. 1A and B). Strains with a reporter protein inserted into domain III of NS5A do not have a defect in RNA replication. However, an ~1.7-log reduction in release of infectious viruses was observed due to the role of NS5A domain III in viral assembly (5) (Fig. 1A and B). This can be mitigated by cell culture adaptations, such as a 40-amino-acid deletion in NS5A domain II (21). Lastly, reporter strains with the reporter protein situated between p7 and NS2 produce infectious virions (22), but again with a reduction in infectivity (23).

To create a more infectious Jc1 reporter strain, we used a monocistronic HCV genome with a reporter gene inserted between NS5A and NS5B. Flanking NS5A/NS5B cleavage sites around the reporter gene allowed the viral NS3/4A protease to release the reporter from the viral polyprotein. The Jc1/$^{NS5AB\text{-}GFP}$ and Jc1/$^{NS5AB\text{-}mKO2}$ (mKO2 [monomeric Kusabira Orange 2 fluorescent protein]) strains displayed nearly unaltered virus titers from the untagged Jc1 virus and much higher titers than existing monocistronic (Jc1/$^{NS5A\text{-}GFP}$) or bicistronic (GFP-Jc1) reporter strains (Fig. 1B; see also Fig. S1 in the supplemental material). Accordingly, viral RNA in supernatants of Jc1/^{NS5AB}-transfected cells was similar to that of untagged Jc1, and ~5-fold higher than Jc1/$^{NS5A\text{-}GFP}$ or GFP-Jc1 strains (Fig. 1C).

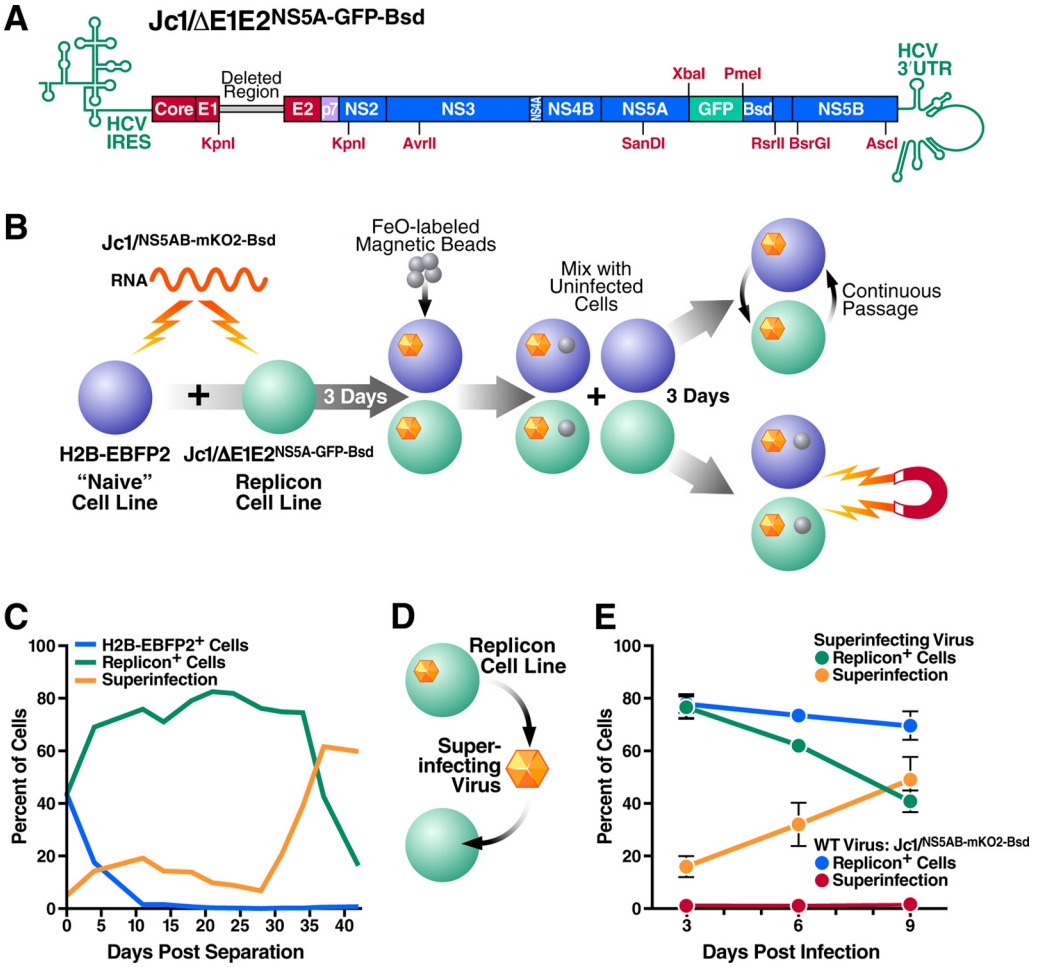

FIG 2 Isolation of a superinfectious HCV strain. (A) Schematic diagram of the Jc1/ΔE1E2$^{NS5A\text{-}GFP}$ replicon construct. (B) Diagram of the strategy used to isolate the superinfectious Jc1/$^{NS5AB\text{-}mKO2\text{-}Bsd}$ reporter strain. Briefly, a 1:1 mixture of HCV-naive EBFP2-tagged cells (H2B-EBFP2) and polyclonal Jc1/ΔE1E2$^{NS5A\text{-}GFP}$ replicon-containing cells were transfected with Jc1/$^{NS5AB\text{-}mKO2\text{-}Bsd}$ RNA. Three days later, these cells were labeled with FeOLabel magnetic beads and mixed with unlabeled H2B-EBFP2 and Jc1/ΔE1E2$^{NS5A\text{-}GFP}$ cells to allow the secondary Jc1/$^{NS5AB\text{-}mKO2\text{-}Bsd}$ virus to spread into the unlabeled cells. The magnetically labeled cells were removed 3 days later, and the Jc1/$^{NS5AB\text{-}mKO2\text{-}Bsd}$-infected culture was continuously passaged. (C) Emergence of a superinfectious Jc1/$^{NS5AB\text{-}mKO2\text{-}Bsd}$ strain during continuous passage. The blue line indicates the percentage of H2B-EBFP2 "naive" cells determined by flow cytometry; these cells were quickly eliminated from the culture, likely by the Jc1/$^{NS5AB\text{-}mKO2\text{-}Bsd}$ virus. The orange line indicates the percentage of Jc1/ΔE1E2$^{NS5A\text{-}GFP}$ replicon-containing cells superinfected with Jc1/$^{NS5AB\text{-}mKO2\text{-}Bsd}$. Note that emergence of the superinfectious strain at ~27 days after separation correlates with elimination of the Jc1/ΔE1E2$^{NS5A\text{-}GFP}$ replicon (green line) from the culture. (D) Serial passage of viral supernatants over replicon-containing cultures to further select for a superinfectious phenotype. (E) Viral supernatants passaged for 10 rounds display high superinfection rates and the ability to exclude the primary replicon. WT or adapted (10 rounds of passage over replicon cells) Jc1/$^{NS5AB\text{-}mKO2\text{-}Bsd}$ viruses were used to superinfect polyclonal Jc1/ΔE1E2$^{NS5A\text{-}GFP}$ replicon-containing cells. The percentage of superinfected replicon$^+$ cells and the total percentage of replicon$^+$ cells were measured by flow cytometry at the given time points. $n = 3$ independent experiments; error bars indicate the SEM.

However, distinguishing infected and uninfected populations with Jc1/$^{NS5AB\text{-}GFP}$ and Jc1/$^{NS5AB\text{-}mKO2}$ was difficult by flow cytometry (see Fig. S1 in the supplemental material). We found that by fusing a blasticidin resistance gene (Bsd) to mKO2 (Jc1/$^{NS5AB\text{-}mKO2\text{-}Bsd}$), we obtained a brighter fluorescent signal from infected cells, and the virus was still 1-log more infectious than Jc1/$^{NS5A\text{-}GFP}$ and GFP-Jc1 (Fig. 1B; see Fig. S1 in the supplemental material). It is not clear why including the Bsd gene increased the fluorescence intensity; blasticidin was not added to the culture. We elected to use the Jc1/$^{NS5AB\text{-}mKO2\text{-}Bsd}$ virus in further experiments as we considered clear discrimination of infected cells of paramount importance.

Emergence of a superinfectious variant of HCV correlates with the exclusion of the primary replicon. To select for a superinfectious strain of HCV, we first attempted to superinfect Jc1/ΔE1E2$^{NS5A\text{-}GFP\text{-}Bsd}$ polyclonal replicon cells (Fig. 2A) with Jc1/$^{NS5AB\text{-}mKO2\text{-}Bsd}$ viral supernatants. However, viral supernatants provide only a single pulse of infection; additionally, cell-free virus transmission is less efficient than cell-cell transmission (24). Correspondingly, only a very small number of replicon cells were superinfected, and the Jc1/$^{NS5AB\text{-}mKO2\text{-}Bsd}$ secondary infection was quickly eliminated from cultures (data not shown).

Therefore, rather than simply passage viral supernatants onto new cultures, we preserved the most efficient method of infection, cell-to-cell spread. To do this, cells in the primary

TABLE 1 Sequence analysis of point mutations in round 1 and round 9 supernatant passages of superinfectious virus

	HC/J6 derived sequence					JFH-1 derived sequence						
HCV gene[a]	E1	E1	E2	E2	p7	NS3	NS4A	NS5A	NS5A	NS5A	Bsd	3′UTR poly(U/UC)
Nucleotide no.												
Jc1/NS5AB-mKO2-Bsd	1087	1343	1571	1637	2607	5030	5412	7159	7160	7649	8525	10701
H77 reference (AF009606)	1088	1344	1572	1638	2596	5019	5401	7160	7161	7586	N/A	N/A
Construct nucleotide	G	G	A	T	T	G	A	G	T	G	T	C
Mutant prevalence*												
Round 1		T/g			T/c		T	A/g	C/t		C	T
Round 9	A/g	T	G	C/T	C/t	A	T	A	C	A/G	C	T
Round 1 distribution†												
Mutant		6/8			3/7		10/10	7/11	7/11		7/7	9/9
Round 9 distribution												
Mutant	8/10	4/4	6/6	3/6	8/12	6/6	6/6	6/6	6/6	3/6	5/5	4/4
Amino acid no.												
Jc1/NS5AB-mKO2-Bsd	249	335	411	433	756	1564	1691	2273	2274	2437	2729	N/A
H77 reference (AF009606)	249	335	411	433	752	1560	1687	2273	2274	2415	N/A	N/A
Amino acid change	Silent	A→S	I→V	Silent	V→A	A→T	H→L	Silent	C→R	D→N	Y→H	N/A

[a] *, Mutant prevalence in sequenced clones is indicated as follows: X/X (50/50 distribution), X/x (major/minor nucleotide), and X (fixed mutation), (mutation not observed). †, Mutant distribution is indicated as the number of sequenced clones with/without the mutation. For the poly(U/UC) mutation, a number of round 1 and 9 clones had a deletion in this region and do not contribute to these numbers.

Jc1/$^{NS5AB\text{-}mKO2\text{-}Bsd}$-transfected culture were labeled with paramagnetic FeOLabel beads and mixed with an equal number of cells in the secondary untransfected culture. After allowing the infection to spread into the secondary culture for 3 days, we removed the cells from the primary culture by magnetic selection (Fig. 2B). In pilot experiments, we found that 83% of FeOLabel-transfected cells could be removed by magnetic selection 3 days after coculture (data not shown).

We also elected to mix an equal number of replicon-negative "naive" cells with the replicon cells to act as a reservoir of virus that could spread into the replicon cells. 7.5-H2B-EBFP2 cells (containing a histone H2B-enhanced blue fluorescent protein proviral insertion) were used as "naive" cells (17) (Fig. 2B). Cell percentages do not sum to 100% since only ~80% of the Jc1/ΔE1E2$^{NS5A\text{-}GFP\text{-}Bsd}$ replicon cells are positive for green fluorescent protein (GFP$^+$), which is typical of fluorescently tagged JFH-1 based replicons under antibiotic selection (25).

Our initial plan was to gradually decrease the ratio of naive to replicon cells through multiple rounds of coculture and magnetic separation in order to gradually increase the selection pressure to superinfect. A similar strategy was used to isolate protease inhibitor-resistant HCV strains (26). However, we found that multiple rounds of coculture, followed by magnetic selection, were unnecessary for two reasons. First, after the first round of this viral "passage" between cultures, the naive 7.5-H2B-EBFP2 cells were gradually eliminated from the culture, likely due to HCV infection-induced death from the Jc1/$^{NS5AB\text{-}mKO2\text{-}Bsd}$ virus. Second, a low-level but stable superinfection, as measured by the percentage of replicon-positive cells that were also Jc1/$^{NS5AB\text{-}mKO2\text{-}Bsd}$ positive, was established in the replicon-containing cells (Fig. 2C).

By simply continuing to passage the cells in this culture, we observed the emergence of a Jc1/$^{NS5AB\text{-}mKO2\text{-}Bsd}$ variant that superinfected replicon cells to high levels beginning 31 days after magnetic separation, as measured by the large increase in GFP$^+$ mKO2$^+$ cells. Remarkably, emergence of the superinfecting strain correlated with the disappearance of replicon-positive cells in the culture (Fig. 2C), suggesting that the secondary virus was excluding active replication of the primary replicon.

Sequence analysis of the superinfectious Jc1 strain reveals adaptive mutations and deletions. We hypothesized that the superinfectious Jc1 strain acquired novel mutations that correlate with superinfectivity. The sequence of the superinfectious strain's genome was analyzed by isolating RNA from viral supernatants from the continuously passaged culture 42 days after magnetic separation. The RNA was reverse transcribed and PCR amplified in eight segments spanning the entire Jc1/$^{NS5AB\text{-}mKO2\text{-}Bsd}$ genome. The primers used for amplification are given in Table S1 in the supplemental material (the extreme 5′- and 3′-terminal regions were not amplified). We then cloned the PCR products and sequenced them. To determine which mutations had been acquired by the superinfectious strain ("round 1"; Table 1), we hoped to specifically sequence the Jc1/$^{NS5AB\text{-}mKO2\text{-}Bsd}$ rather than the Jc1/ΔE1E2$^{NS5A\text{-}GFP\text{-}Bsd}$ genome. Packaging of defective HCV genomes occurred when E1E2 is expressed *in trans*, although with a 100-fold reduction in infectivity compared to *cis*-packaging (27). Fortunately, few of the clones had sequences derived from the Jc1/ΔE1E2$^{NS5A\text{-}GFP\text{-}Bsd}$ replicon. Jc1/ΔE1E2$^{NS5A\text{-}GFP\text{-}Bsd}$ sequences would manifest as a deletion in E1/E2 or a GFP-Bsd insertion in NS5A domain III. No clones had NS5A-GFP-Bsd sequence, and only 2/16 clones had the ΔE1E2 sequence.

We hypothesized that further selection pressure for superinfectivity would lead to fixation of the mutations acquired in round 1, as well as the acquisition of further adaptive mutations. The superinfectious virus could now be directly passaged over Jc1/

TABLE 2 Sequence analysis of deletions in round 1 and round 9 supernatant passages of superinfectious virus[a]

Clone	mKO2-Bsd deletion		Poly(U/UC) deletion		Poly(U) tract length (nt)	
	Round 1	Round 9	Round 1	Round 9	Round 1	Round 9
1	7733–8623	8586–8798	10716–10739	10716–10739	40	63
2	7733–8623	8586–8795	10716–10739	10716–10739	41	45
3	7677–8822	8586–8795	10716–10739	10716–10739	65	50
4	7677–8822	8589–8798	10716–10739	10716–10739	41	45
5	ND	8589–8798	10716–10739	10716–10739	45	36
6	ND	8525–8562, 8584–8799	10716–10739	—	39	35
7	ND	—	10716–10739	—	50	—
8	ND	—	10716–10739	—	54	—
9	ND	—	10716–10739	—	50	—
10	ND	—	10716–10739	—	41	—
11	ND	—	10716–10739	—	52	—
12	ND	—	10716–10739	—	50	—
13	ND	—	10716–10739	—	63	—
14	ND	—	10716–10739	—	65	—
15	ND	—	—	—	—	—
16	ND	—	—	—	—	—
17	ND	—	—	—	—	—
18	ND	—	—	—	—	—
Median					50	45

[a] ND, no deletion; –, not a sequenced clone.

ΔE1E2$^{NS5A\text{-}GFP\text{-}Bsd}$ replicon cells, by serial passage of viral supernatants (Fig. 2D and E). This was not possible with wild-type (WT) Jc1/$^{NS5AB\text{-}mKO2\text{-}Bsd}$, since the secondary virus does not persist due to superinfection exclusion. The superinfectious virus was passaged for nine rounds over Jc1/ΔE1E2$^{NS5A\text{-}GFP\text{-}Bsd}$ replicon cells to provide further selection pressure for the ability to superinfect. The viral RNA was again sequenced, expanding the sequenced region to the full 5′- and 3′-terminal regions (see Table S1 in the supplemental material). Again, only 1/7 clones had the ΔE1E2 sequence, and none had the NS5A-GFP-Bsd sequence (alignments are provided of round 1 and round 9 sequences in data sets S1 and S2, respectively, in the supplemental material).

Point mutations present in at least 50% of clones sequenced in either round 1 or 9 are shown in Table 1. We observed seven nonsynonymous mutations leading to an amino acid change and three silent mutations in the viral coding sequence. The distribution of deletions in the various clones analyzed is shown in Table 2. In round 1, deletions spanning much of the mKO2-Bsd region were observed in 4 of 18 clones. In passaging viral supernatants, cultures were selected for high numbers of mKO2$^+$ replicon$^+$ cells, whereas blasticidin was not used for selection. Correspondingly, in round 9, 5/5 clones had deletions in the Bsd gene, but no clones had deletions in mKO2. A specific deletion of 24 nucleotides (nt) in the poly(U/UC) region of the 3′UTR was observed in all clones analyzed.

Viral adaptive mutations increase HCV superinfectivity. How do these point mutations and poly(U/UC) deletion affect superinfectivity? To examine this, we introduced the seven amino acid substitutions in the viral coding sequence and a 21-nt deletion in the poly(U/UC) into the parental Jc1/$^{NS5AB\text{-}mKO2\text{-}Bsd}$ construct (the observed deletions in mKO2-Bsd were not introduced). Our initial studies showed that the NS5A D2437N mutation in the protease cleavage site between NS5A and mKO2-Bsd was detrimental to superinfectivity (data not shown). This is not surprising, since this is a change from a highly conserved—but not essential (28)—acidic residue in the P6 position of the NS5A/mKO2-Bsd cleavage site. Correspondingly, this mutation was analyzed separately. The mutant and parental WT Jc1/$^{NS5AB\text{-}mKO2\text{-}Bsd}$ viruses were used to superinfect Jc1/ΔE1E2$^{NS5A\text{-}GFP\text{-}Bsd}$ replicon cells. The viral input was normalized as the amount of HCV core per infection, which did not appreciably vary across the mutant strains after viral production (data not shown). The Mut7 virus, carrying the poly(U/UC) deletion and 6 of 7 of the amino acid substitutions, was ~15-fold as superinfectious as the WT strain (Fig. 3B). Note that including the NS5A D2437N mutation leads to a defect in superinfectivity.

We next analyzed the contribution of the Mut7 mutations to superinfectivity by reverting each of the mutations to WT and used the resulting viruses to infect Jc1/ΔE1E2$^{NS5A\text{-}GFP\text{-}Bsd}$ replicon cells. The E1 A335S, p7 V756A, and NS5A C2274R mutations appeared to be the most important (Fig. 3B) since their reversion to WT caused a decrease in superinfectivity. To ensure that the superinfectious phenotype of these viruses was not limited to the same polyclonal Jc1/ΔE1E2$^{NS5A\text{-}GFP\text{-}Bsd}$ replicon cell line used for initial selection of the virus, infections were also carried out in a separately transfected and isolated monoclonal Jc1/ΔE1E2$^{NS5A\text{-}GFP\text{-}Bsd}$ replicon cell line. No difference in superinfection was observed between the polyclonal and monoclonal replicon cell lines. Viral strains lacking the E1 A335S, p7 V756A, and NS5A C2274R mutations were also less capable of superinfecting monoclonal Jc1/ΔE1E2$^{NS5A\text{-}GFP\text{-}Bsd}$ replicon cells when viral input was normalized to infectious titer (Fig. 4).

The various mutant strains of Jc1/$^{NS5AB\text{-}mKO2\text{-}Bsd}$ were then used to infect naive Huh7.5 cells and genotype 1b replicon cells. Interestingly, mutant viral strains with higher superinfectivity in Jc1/ΔE1E2$^{NS5A\text{-}GFP\text{-}Bsd}$ replicon cells had higher infectivity in naive Huh7.5 cells (Fig. 3B and C). Superinfection studies were also performed in the Con1 SGR/$^{NS5A\text{-}GFP}$ genotype 1b replicon cell line (Fig. 3A and D). This replicon, containing the NS5A S1179I adaptive mutation (29), displayed low levels of GFP$^+$ cells even

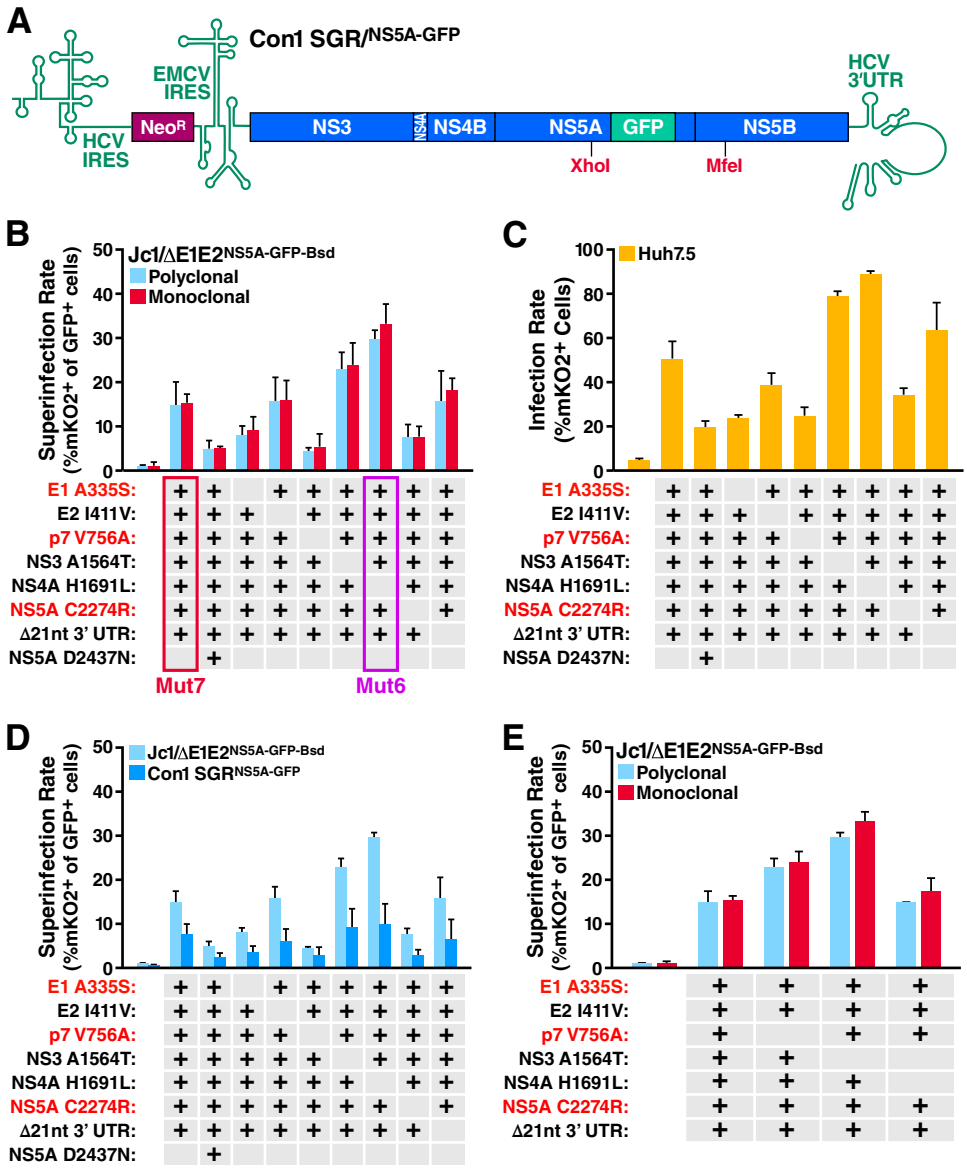

FIG 3 Contribution of identified mutations to the superinfectious phenotype. (A) Schematic diagram of the genotype 1b Con1 SGR/$^{NS5A-GFP}$ replicon. Neo^{R} indicates the neomycin resistance gene. (B) Recapitulation of the superinfectious phenotype with seven mutations. Mutations were introduced into the WT Jc1/$^{NS5AB-mKO2-Bsd}$ construct, and viral supernatants were produced by transfection of these variants into Huh7.5 cells. Supernatants were normalized to the quantity of HCV core (determined by ELISA) and Jc1/ΔE1E2$^{NS5A-GFP}$ replicon-containing cells were superinfected. The percent superinfection was assessed by flow cytometry 3 days later. To ensure that the superinfectious phenotype was not limited to a particular Jc1/ΔE1E2$^{NS5A-GFP}$ replicon cell line, superinfections were performed in polyclonal and monoclonal replicon cells (replicon cell lines were isolated separately). Note that the NS5A D2437N mutation had a detrimental effect on superinfectivity and was thus excluded from the majority of variants analyzed. (C) Superinfectivity correlates with a higher degree of infectivity in naive cells. The same viruses used in panel A were used to infect naive Huh7.5 cells. (D) Superinfection is reduced in a genotype 1b replicon cell line. Polyclonal Jc1/ΔE1E2$^{NS5A-GFP}$ and Con1 SGR/$^{NS5A-GFP}$ replicon cells were superinfected with the given viral variants. (E) Both NS3 A1564T and NS4A H1691L increase superinfectivity alone but not when the mutations were combined. $n = 4$ independent viral preparations and infections; error bars indicate the SEM.

after G418 selection. Hence, Con1 SGR/$^{NS5A-GFP}$ replicon cells were enriched once by FACS sorting for GFP^{+} cells before experimental use, as in previous studies (30). As anticipated, higher superinfectivity in Jc1/ΔE1E2$^{NS5A-GFP-Bsd}$ replicon cells correlated with higher superinfectivity in Con1 SGR/$^{NS5A-GFP}$ replicon cells. Unexpectedly, the superinfectivity of adapted strains was generally lower in the Con1 SGR/$^{NS5A-GFP}$ replicon cells. One possibility for this result is that the superinfectious virus may have evolved to specifically superinfect cells replicating genotype 2a HCV RNA.

We were intrigued that reverting either the NS3 A1564T or the NS4A H1691L mutation led to an increase in superinfectivity (Fig. 3B). We therefore reverted both mutations together to the WT sequence and superinfected Jc1/ΔE1E2$^{NS5A-GFP-Bsd}$ replicon cells with this virus (Fig. 3E). Surprisingly, reverting both mutations did not lead to a further increase in superinfectivity; instead, superinfectivity was lower than in the single revertants. We therefore conclude that the NS3 A1564T and NS4A H1691L mutations increase superinfectivity in isolation but not in conjunction.

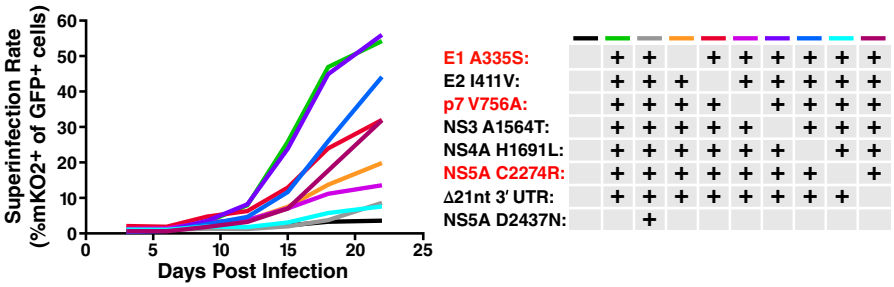

FIG 4 Superinfection spread in replicon cells demonstrates the importance of E1 A335S, p7 V756A, and NS5A C2274R mutations. Jc1/ΔE1E2$^{NS5A\text{-}GFP}$ monoclonal replicon-containing cells were superinfected at a multiplicity of infection of 0.1 (7.5×10^4 FFU/ml), and cultures were continuously passaged for 22 days-postinfection. The superinfection rate (%mKO2$^+$ of GFP$^+$ cells) was analyzed at various time points by flow cytometry. Note that the superinfectious phenotype is still present even when viral input is normalized by infectious titer rather than HCV core; a long period of viral spread, however, is required to observe this phenotype. The data are representative of three independent viral preparations and experiments.

Adaptive mutations promote superinfectivity in a nonreporter Jc1 strain. Is the increase in infectivity and superinfectivity afforded by the Mut7 and Mut6 mutations limited to the Jc1/$^{NS5AB\text{-}mKO2\text{-}Bsd}$ or Jc1/$^{NS5AB\text{-}Barcode}$ reporter strains of the virus? We introduced the Mut7 and Mut6 virus mutations (Fig. 3B) into a nonreporter Jc1 strain to ensure this was not the case. Indeed, when analyzing viral infectivity in supernatants of transfected Huh7.5 cells, we observed a 1- and 1.5-log increase in infectivity for the Mut7 and Mut6 virus, respectively, compared to WT Jc1 (Fig. 5A).

Analysis of superinfection of replicon-containing cells is difficult in the absence of a reporter for the secondary virus, since the Jc1/ΔE1E2$^{NS5A\text{-}GFP\text{-}Bsd}$ replicon causes the cells to immunostain positive for viral proteins (excepting E1 and E2) and dsRNA. It would be possible to use an NS3-NS5B subgenomic replicon and stain for a viral protein such as NS2 to measure superinfection. However, because the highly superinfectious virus excluded the primary replicon from cells (Fig. 2C and E), we were able to use this exclusion as an indirect means of measuring superinfection efficiency in nonreporter Jc1 strains. We superinfected Jc1/ΔE1E2$^{NS5A\text{-}GFP\text{-}Bsd}$ polyclonal replicon cells with Mut6, Mut7, and WT nonreporter Jc1, as well as with the superinfecting Jc1/$^{NS5AB\text{-}mKO2\text{-}Bsd}$ strain (rounds 10, 11, and 13). The primary replicon (%GFP$^+$ cells) was rapidly excluded when cells were superinfected with Mut7 or Mut6 Jc1 compared to WT Jc1 or uninfected cells (Fig. 5B). Similarly, we superinfected 7.5-RLuc Jc1/ΔE1E2$^{NS5A\text{-}FLuc\text{-}Bsd}$ polyclonal replicon cells with Mut6, Mut7, and WT nonreporter Jc1. These cells express firefly luciferase (FLuc) from the viral replicon and a *Renilla* luciferase (RLuc) cellular control from a lentiviral proviral insertion. As demonstrated by the decrease in the FLuc/RLuc ratio, the primary replicon replication level was lower when cells were superinfected with Mut7 or Mut6 Jc1 compared to WT Jc1 or uninfected cells (Fig. 5C).

Tracking viral variants using sequence barcodes. We sought to further analyze how these adaptive mutations affected viral dynamics and superinfectivity when the highly fit Mut7 and each of the seven single revertant strains were allowed to compete with each other. By coinfecting Huh7.5 cells with different viral strains, the strain capable of superinfecting at higher efficiency should eventually dominate due to superinfection and exclusion of the less-fit strain from host cells.

However, to compare each combination of Mut7, the single revertants, and wild-type Jc1 would require 72 separate coinfections. A more straightforward means of performing these comparisons would be to simply coinfect with all nine of these viruses simultaneously and analyze which viral genome(s) dominate at a later time point in the culture. The difficulty with this approach arises in identifying which of the nine viral strains dominates. It is not possible to use different fluorescent tags (e.g., EBFP2, GFP, mKO2) in each of the viral strains; nine fluorescent proteins that are resolvable by flow cytometry do not exist. In addition, the different sizes and amino acid sequences of the fluorescent proteins could confound analysis by altering the fitness of the virus (e.g., Jc1/$^{NS5AB\text{-}mKO2\text{-}Bsd}$ is less fit than Jc1/$^{NS5AB\text{-}mKO2}$; Fig. 1).

We elected to instead label each viral strain with a 12-nt RNA sequence tag, or barcode (31), inserted between NS5A and NS5B to create Jc1/$^{NS5AB\text{-}Barcode}$ strains (Fig. 6). The barcodes were varied using silent mutations; thus, the amino acid sequence is the same for each barcode, and no differential effects on viral fitness should occur. Each barcode differs from every other barcode at three or more positions, allowing clear discrimination of barcodes even in the instance of point mutations.

Identification of viral barcodes was performed by isolation of viral RNA from supernatants, and initial RT-PCR amplification of a 538-nt amplicon. The barcode tags were then reamplified using a nested PCR comprising a 74-nt or an 86-nt amplicon. The nested PCR approach was used to reduce the possibility of PCR contamination due to the small size of the second amplicon and the low input of viral RNA. To reduce sequencing effort and expense, the barcodes were concatenated using complementary fusion adaptors at the 5′ end of the primers (32). Overlap extension of the adaptors during the nested PCR fused the barcodes into long concatemers, which were then cloned and Sanger sequenced. On average, 6.1 barcodes/sequencing read were obtained using the 86-nt amplicon, and 7.1 barcodes/sequencing read were obtained using the 74-nt amplicon. The higher barcode yield with the 74-nt amplicon was likely due to the shorter nucleotide span between concatenated barcodes (41 nt compared to 59 nt) but was still below the theoretical ~14 barcodes possible for an 800-nt sequencing read (see notes in the supplemental results). On average, 62.7 barcodes were sequenced for each experimental data point, totaling 2,258 barcodes (Fig. 7A to C). When using defined mixtures of the nine viral RNAs, the barcode sequencing approach was quite accurate at measuring the relative proportion of each, as shown in Fig. 7A, columns 1 and 2.

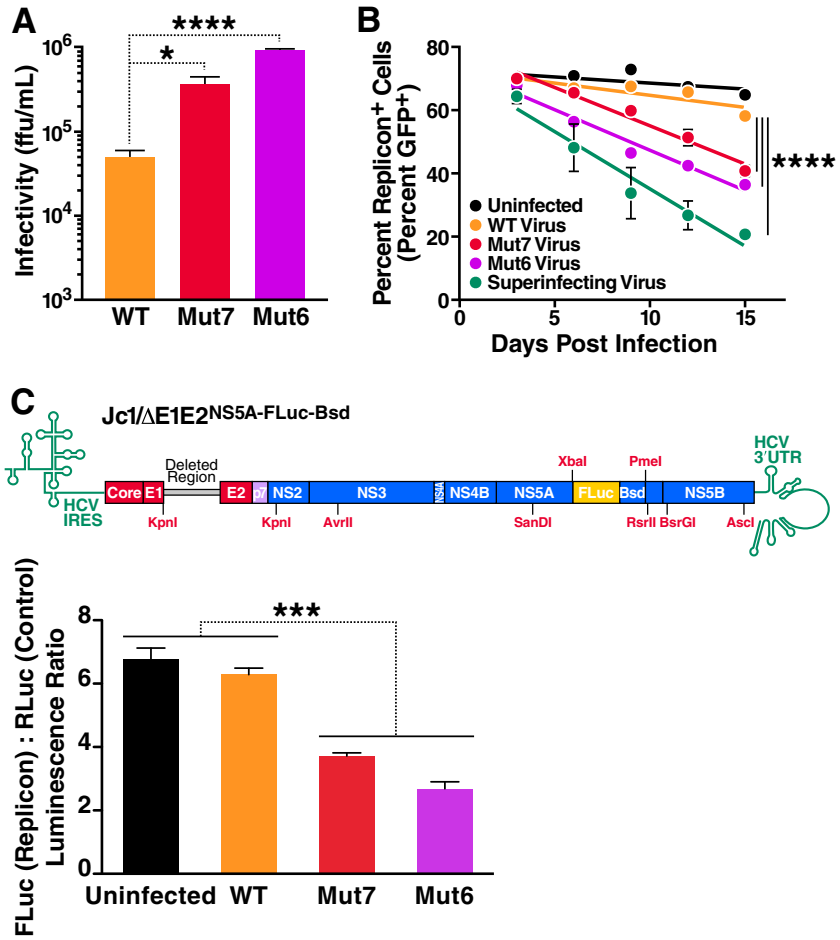

FIG 5 The highly infectious and superinfectious phenotype of the Mut7 and Mut6 viruses is not limited to the Jc1/$^{NS5AB\text{-}mKO2\text{-}Bsd}$ reporter strain. (A) Infectivity of supernatants from Mut7 and Mut6 Jc1-transfected cultures is ~10-fold higher than WT Jc1-transfected cultures. Untagged Jc1 (WT, Mut7, or Mut6) viral supernatants produced by transfection of Huh7.5 cells were assessed for infectivity using the limiting dilution assay on naive Huh7.5 cells. (B) Exclusion of the Jc1/ΔE1E2$^{NS5A\text{-}GFP}$ primary replicon is enhanced in Mut7- and Mut6-superinfected cultures. Polyclonal Jc1/ΔE1E2$^{NS5A\text{-}GFP}$ replicon-containing cells were superinfected with untagged Jc1 (WT, Mut7, or Mut6) or the adapted superinfecting strain (rounds 10, 11, and 13) viral supernatants. Exclusion of the primary replicon was assessed by flow cytometry. (C) Exclusion of the Jc1/ΔE1E2$^{NS5A\text{-}FLuc\text{-}Bsd}$ primary replicon is enhanced in Mut7- and Mut6-superinfected cultures. Polyclonal 7.5-RLuc Jc1/ΔE1E2$^{NS5A\text{-}FLuc\text{-}Bsd}$ cells were superinfected with untagged Jc1 (WT, Mut7, or Mut6). 6 days postinfection, cells were analyzed for FLuc (replicon-derived) and RLuc (control, lentivirus-derived) luminescence. Note the greater loss of the primary replicon in the Mut7 Jc1 and Mut6 Jc1-superinfected cultures compared to WT Jc1-superinfected or nonsuperinfected cultures. $n = 3$ independent viral preparations and infections; error bars indicate ± the SEM. *, $P < 0.05$; ***, $P < 0.001$; ****, $P < 0.0001$ (one-way ANOVA or analysis of covariance).

Superinfection dynamics in multiply infected cultures. A viral strain with a more superinfectious phenotype should eventually dominate in a mixed infection due to superinfection and concomitant exclusion of the less-fit primary viral strain. Mut7, each of the seven single revertants (not including NS5A D2437N), and WT Jc1/$^{NS5AB\text{-}Barcode}$ strains were used simultaneously in the mixed infections. Initially, we transfected equal amounts each viral RNA simultaneously into Huh7.5 cells in an attempt to establish each strain on an equal standing and allowed the viral strains to spread throughout the culture (Fig. 7A). The relative proportions of each viral strain in the culture were assessed from 3 to 21 days posttransfection by barcode sequencing of viral RNA from cell-free supernatants. Note that adaptation of the viral genomes may occur on this time scale; the barcode prevalence simply demonstrates overall viral fitness and superinfection ability given a particular initial genotype.

By 3 days posttransfection, >70% of the cells in the transfected culture were HCV RNA positive (data not shown). Viral competition and dominance at this point reflects the ability to successfully superinfect neighboring infected cells and exclude the primary viral genome. As expected, the WT virus was quickly excluded from the culture, since it superinfects with low efficiency. Likewise, viral strains lacking the p7 V756A and NS5A C2274R were also excluded; these mutations were shown to be important when superinfecting replicon-containing cells (Fig. 3). The strain lacking the E1 A335S mutation was not as effectively excluded. Much of the viral spread and superinfection was via cell-to-cell transmission under these conditions, and requirements for viral entry are less strict under these conditions (33). Although the p7 V756A mutation was found to be important in both viral competition experiments (Fig. 7) and superinfection of replicon cells (Fig. 3), a postentry block to HCV replication has been clearly established (5, 7, 34). Given that p7 is dispensable for RNA replication but important for viral assembly, it is likely that

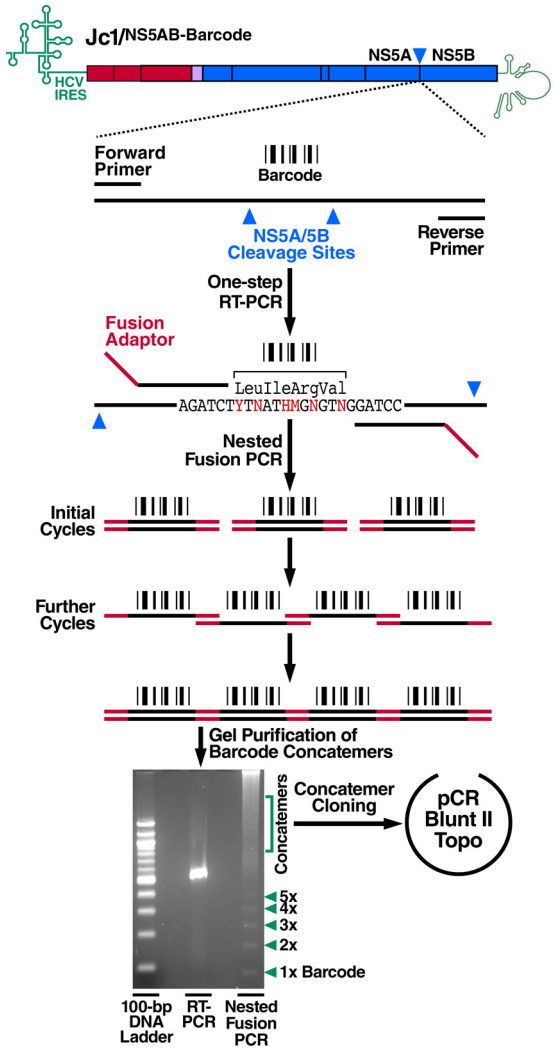

FIG 6 Overview of the viral barcode cloning strategy. Viral RNA was isolated and subjected to one-step RT-PCR using the primers NS5ABmcs_1 and Jc1_Amplicon_15R. A nested PCR was performed using the primers Barcode_LIC_Fw_5 and Barcode_LIC_Rev_5 or the primers Barcode_LIC_Fw_3 and Barcode_LIC_Rev_3. Complementary regions on the 5′ ends of these primers caused the PCR products to anneal at these regions during later cycles; the resulting overlap extension led to the fusion of PCR products into long concatemers. Concatemers were purified by gel extraction and cloned into pCR Blunt II Topo. Colony PCR was then performed, followed by sequencing.

p7 V756A is providing a fitness advantage by increasing the number of infectious viral particles, rather than allowing HCV to overcome the postentry superinfection block.

Of note, the strain lacking the poly(U/UC) deletion was also excluded from the culture; this mutation was not found to be important when superinfecting cells containing a WT replicon (Fig. 3). However, under the mixed infection conditions, the strain lacking the poly(U/UC) deletion is competing to superinfect cells containing highly fit HCV strains. In addition, the barrier to superinfection is likely greater in these experiments due to 5-fold-higher HCV RNA accumulation in acutely infected compared to replicon-positive cells (data not shown). This mutation apparently provides an advantage under these more stringent conditions.

In addition to cotransfecting each of the nine viral RNAs, we coinfected cells simultaneously with a mixture of each of the nine viral strains. This experiment was performed by normalizing each of the viral strains by viral genome input (Fig. 7B), or by infectious titer (Fig. 7C). Note that the viral RNA input under these conditions was determined by quantitative RT-PCR of viral supernatants prior to mixing and is not precisely defined as in Fig. 7A. Importantly, both of the coinfection studies agree with the cotransfection studies; strains lacking p7 V756A, NS5A C2274R, the poly(U/UC) deletion, and the WT strain were excluded from the culture.

HCV strains with a poly(U/UC) deletion and the NS5A C2274R mutation overcome the postentry superinfection block. We next focused our efforts on defining the specific mutations that could act at the postentry step where superinfection exclusion typically occurs (5, 6). The E1, E2, and p7 mutations affect viral entry or assembly and are thus unlikely to play a role. The NS3 and NS4A mutations did not greatly increase superinfectivity and are also unlikely candidates. In contrast, the NS5A C2274R mutation proved important for superinfection (Fig. 3B to D) and increased the amount of viral protein in infected cells (Fig. 8B and C). In addition, we observed that while the poly(U/UC) deletion was dispensable when superinfecting WT replicon-containing cells (Fig. 3), the deletion was important in competition studies with other highly superinfectious strains (Fig. 7). Furthermore, we observed that the median length of the poly(U/UC) tract decreased as the superinfectious virus was passaged over replicon cells (Table 2). Overall, HCV protein levels also increased in cells transfected with viral RNA carrying deletions in the poly(U/UC) (Fig. 8C), a finding consistent with studies demonstrating that a shorter poly(U/UC) increases HCV infectivity *in vitro* (35, 36). These results suggest that the deletion in the poly(U/UC) region and the NS5A C2274R mutation are key to allowing the virus to overcome postentry superinfection exclusion.

We analyzed the effects of the adaptive mutations on overcoming the postentry superinfection block by "supertransfecting" Jc1/ΔE1E2$^{NS5A\text{-}GFP\text{-}Bsd}$ polyclonal replicon cells with equal amounts of various mutant Jc1/$^{NS5AB\text{-}mKO2\text{-}Bsd}$ RNAs. Supertransfection (as opposed to superinfection) of replicon-containing cells focuses specifically on the postentry block, since virion assembly and entry do not play a role. In addition to the 21-nt deletion of the poly(U/UC) in the superinfection studies, viral genomes carrying a 36-nt poly(U/UC) deletion were used (Fig. 8A). Progressively shortening the poly(U/UC) tract caused a corresponding increase in supertransfection (Fig. 9A). By including the NS5A C2274R mutation in the context of the poly(U/UC) deletions, a slight increase in supertransfection was observed. However, when the other Mut7 mutations were included (E1 A335S, E2 I411V, p7 V756A, NS3 A1564T, and NS4A H1691L), we detected no additional increase in supertransfection (Fig. 9A). When these same viral RNAs were used to transfect naive Huh7.5 cells, we observed that a shorter poly(U/UC) increased the transfection efficiency but not to the same extent, due to the high permissivity of naive cells (Fig. 9B).

By superinfecting Jc1/ΔE1E2$^{NS5A\text{-}GFP\text{-}Bsd}$ polyclonal replicon cells with these mutant strains, we again observed that a shorter poly(U/UC) allowed the secondary virus to better-overcome superinfection exclusion (Fig. 9C). Furthermore, there appeared to be a synergistic effect of the shorter poly(U/UC) and the NS5A C2274R mutation on superinfection efficiency. However, we did not observe an effect of the poly(U/UC) deletion on superinfection in the context of the Mut7 mutations. This is likely to result

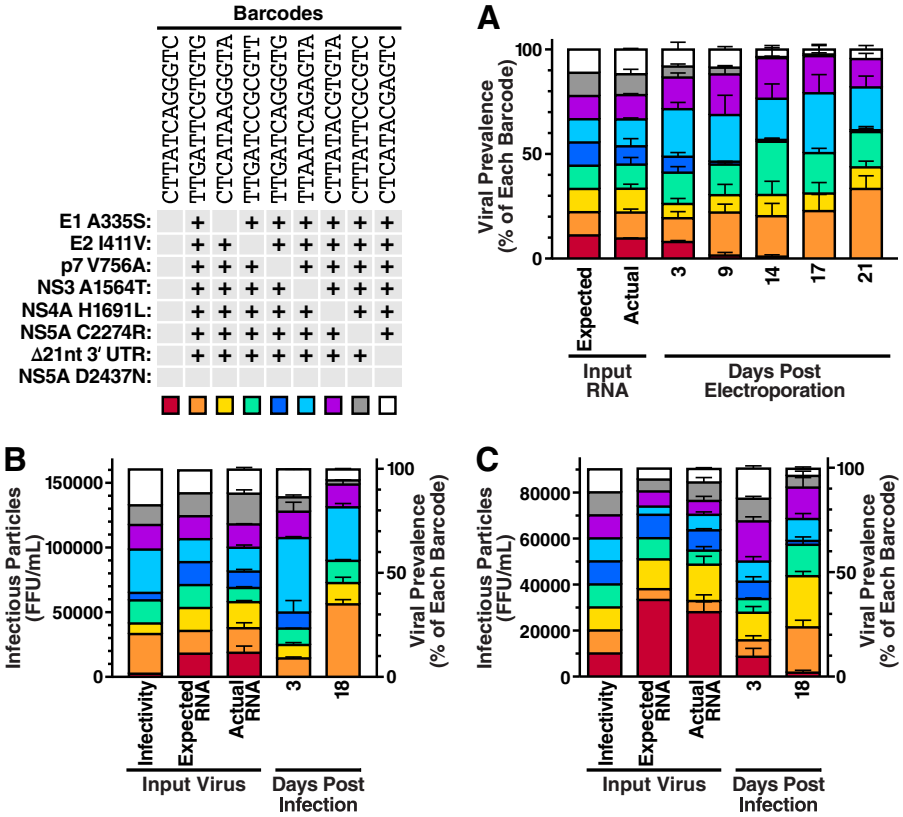

FIG 7 Competition between multiple viral variants shows that p7 V756A, NS5A C2274R, and Δ 3′UTR mutations are important in the superinfectious phenotype. Jc1/^{Barcode} viral strains were introduced into naive Huh7.5 cells by transfection or infection. RNA was obtained from the transfection or infection input or from cell-free supernatants at the given time points posttransfection or postinfection. The relative prevalence of each Jc1/^{Barcode} strain was determined by the barcode cloning strategy shown in Fig. 6. (A) WT Jc1 and strains lacking the p7 V756A, NS5A C2274R, and Δ 3′ UTR mutations are excluded from cotransfected cultures. A total of 1.11 μg of each Jc1/$^{NS5AB\text{-}Barcode}$ viral RNA was cotransfected into Huh7.5 cells. (B and C) The pattern of viral exclusion is similar in coinfected cells, whether viral input is normalized by RNA or infectivity. (B) Viral competition after coinfection with viral stocks normalized by RNA input. Huh7.5 cells were coinfected with 1.53×10^6 viral genome equivalents of each Jc1/$^{NS5AB\text{-}Barcode}$ viral stock/ml. (C) Viral competition after coinfection with viral stocks normalized by infectivity. Huh7.5 cells were coinfected with 1.01×10^4 FFU of each Jc1/$^{NS5AB\text{-}Barcode}$ viral stock/ml. $n = 3$ independent transfections or infections; error bars indicate the SEM.

from the highly infectious phenotype that results from the E1 and p7 mutations, which may allow for sufficiently high entry of the secondary virus to mask the effect of the poly(U/UC) deletion.

Translation of superinfectious viral RNA is unaffected by poly(U/UC) length or the NS5A C2274R mutation. Results from prior studies have been inconsistent on whether superinfection exclusion is mediated in part by a block in translation of secondary viral RNA (5, 6, 37). Since the poly(U/UC) deletion and the NS5A C2274R mutation appear to be key players in overcoming the postentry superinfection block, we chose to assess the effect of these mutations on HCV IRES-mediated translation. RNAs encoding firefly luciferase (FLuc) driven by the HCV IRES were transfected into Jc1/ΔE1E2$^{NS5A\text{-}GFP\text{-}Bsd}$ monoclonal replicon cells, as well as a replicon-cured variant of this cell line (cured by IFN-α treatment). 5′-7-Methyl-guanosine-capped and 3′-polyadenylated *Renilla* luciferase (RLuc) RNA was cotransfected as a transfection control, and luciferase activity was assessed 2 h posttransfection. Deletions in the poly(U/UC) tract of the 3′UTR did not appear to have any effect on translation, although including the 3′UTR did greatly enhance translation (Fig. 10A). Furthermore, no difference was observed in replicon-containing and replicon-cured cells.

We assessed the effect of a shorter poly(U/UC) and the NS5A C2274R mutation on HCV IRES-mediated translation in a more relevant context by introducing these mutations into Jc1/$^{NS5AB\text{-}FLuc}$-GND constructs. The NS5B GND mutation ensures that viral RNA replication cannot occur (38); therefore, FLuc luminescence will only reflect viral RNA translation. Viral RNA translation was not increased as a result of the mutations; if anything, the 21-nt deletion decreased translation (Fig. 10B). Interestingly, viral RNA translation was ~2-fold greater in replicon cells than in replicon-cured cells. We did not observe this effect with the minimal 5′UTR-FLuc-3′UTR constructs, suggesting that replicons enhance HCV IRES-mediated translation specifically in the context of the full-length viral sequence. Combined with this observation, the failure of the poly(U/UC) deletion and NS5A C2274R mutations to enhance HCV IRES-mediated translation suggests that postentry superinfection exclusion does not result from a block in secondary viral RNA translation.

DISCUSSION

In this study, we used highly infectious, Jc1/^{NS5AB} fluorophore-tagged HCV genomes to select for a variant of HCV capable of high levels of superinfection. We found that the emergence of

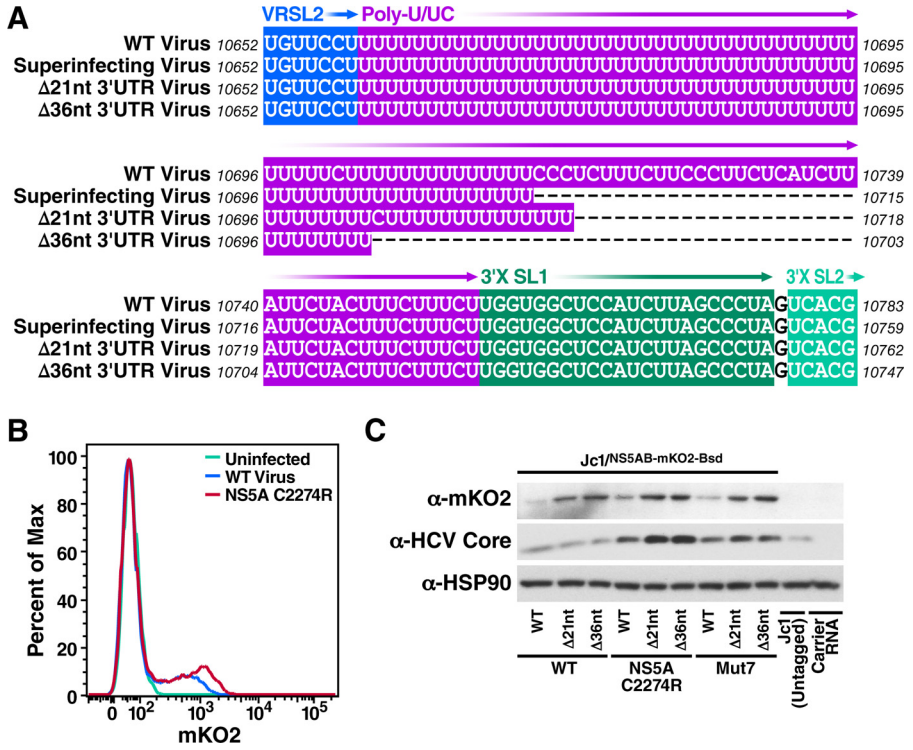

FIG 8 NS5A C2274R and Δ 3′UTR mutations increase the amount of viral protein. (A) Sequence alignment of poly(U/UC) sequences from mutant and WT viral variants. The sequence from the superinfecting virus reflects the 24-nt deletion found in all sequenced clones; the length of the poly(U) tract varied according to each clone. Nucleotides are numbered according to the Jc1/$^{NS5AB\text{-}mKO2\text{-}Bsd}$ RNA. (B) Representative flow cytometry plot indicating an increase in the mean fluorescence intensity of mKO2 in Huh7.5 cells infected with WT or NS5A C2274R Jc1/$^{NS5AB\text{-}mKO2\text{-}Bsd}$. Cells were infected with viral stocks normalized by core input and analyzed by flow cytometry at 3 days postinfection. (C) Western blots indicating an increase in HCV core and mKO2-Bsd in Huh7.5 cells transfected with HCV Jc1/$^{NS5AB\text{-}mKO2\text{-}Bsd}$ strains carrying the NS5A C2274R and Δ 3′ UTR mutations. Cells were transfected with 10 μg of viral RNA, and lysates were obtained 3 days posttransfection.

superinfectivity increases the fitness of the virus generally and that superinfectious viruses can exclude the primary infection. The superinfectious phenotype of a virus also depends on the primary infection; the virus we isolated was far more capable of superinfecting genotype 2a compared to genotype 1b replicon-containing cells. We identified specific adaptive mutations that allow HCV to overcome the postentry barrier to superinfection, namely, a deletion in the poly(U/UC) tract and a C2274R mutation in NS5A. Lastly, we demonstrate that these adaptive mutations do not alter translation of HCV RNA and that superinfection exclusion generally is not caused by a block in the translation of the secondary viral RNA.

We demonstrate that Jc1/^{NS5AB}-tagged genomes display infectious titers more closely resembling untagged Jc1 than the commonly used bicistronic and NS5A domain-III fusion-tagged Jc1 reporter genomes (Fig. 1B) (5, 15, 20). Similar Jc1/^{NS5AB} fluorophore–tagged genomes were recently described by Horwitz et al. (11). In Horwitz et al., a Ypet tag was inserted between NS5A and NS5B bracketed by short NS3/4A cleavage sites (DTTVCC/SM); we used longer cleavage sites (SEEDDTTVCC/SMSYS). In contrast to those findings, we observed incomplete cleavage between NS5A and the fluorophore tag (data not shown). Further, after 11 passages of infected cells (Fig. 2C), we observed that only 4/18 (22%) of the sequenced viral genomes have deletions in the fluorophore tag (Table 2), while Horwitz et al. observed that ~50% of infected cells lose fluorophore-derived fluorescence after only six passages. However, our publications agree on the main finding that high-titer Jc1 reporter strains can be obtained by insertion of the reporter between NS5A and NS5B.

We also devised a novel strategy of investigating viral dynamics in cultures infected with multiple HCV strains simultaneously. Previous studies have sequence barcoded up to 6,200 yeast (39, 40) or viral (39, 40) strains for competition experiments and analyzed the barcodes by deep sequencing (Bar-seq) or microarrays. As we were competing a relatively small number of viral strains (nine), we identified the barcodes using an approach based on the principles of serial analysis of gene expression (SAGE) (41). The sequence barcodes were fused into concatemers in a simple two-step PCR, cloned, and identified by Sanger sequencing. This approach provides a labor and cost advantage over barcode microarrays and Bar-seq when comparing the fitness of a relatively small number of HCV strains (42). Furthermore, since discrete, countable tags are sequenced, direct comparison between multiple time points or conditions in a single experiment are possible (Fig. 7A). Microarrays can only directly compare two conditions. Our serial analysis of barcode expression (SABE) approach may be useful in comparing the fitness of a small number of HCV strains with different combinations of drug resistance mutations in response to drug treatment. When comparing many viral strains, the number of barcode sequences required scales up rapidly; Bar-seq is more appropriate under these conditions, since the cost of Sanger sequencing will quickly become prohibitive.

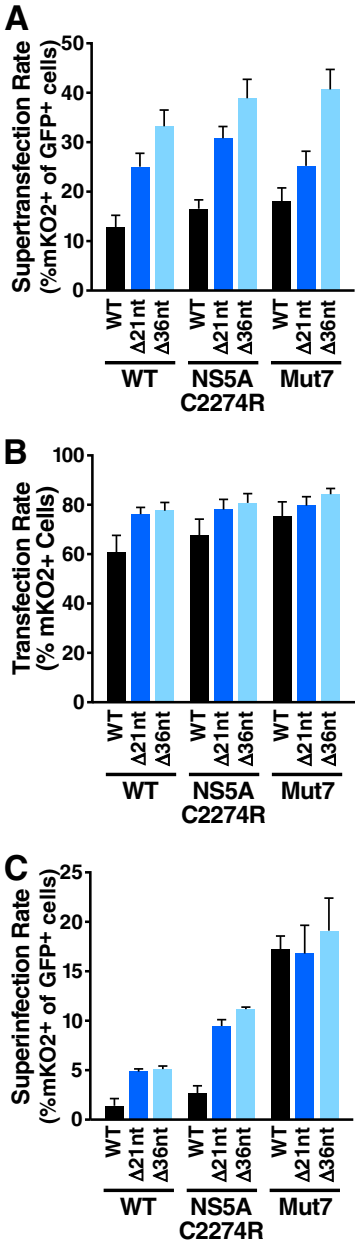

FIG 9 NS5A C2274R and Δ 3′UTR mutations increase "supertransfection" in replicon-containing cells. (A) "Supertransfection" is greatly enhanced by poly(U/UC) deletions and slightly enhanced by the NS5A C2274R mutation. Jc1/ΔE1E2$^{NS5A\text{-}GFP}$ polyclonal replicon cells were transfected with WT and mutant Jc1/$^{NS5AB\text{-}mKO2\text{-}Bsd}$ transcripts. The "supertransfection" rate was assessed by flow cytometry as the percentage of replicon-positive cells (GFP$^+$) that were also positive for the secondary Jc1/$^{NS5AB\text{-}mKO2\text{-}Bsd}$ virus (mKO2$^+$) 2 days posttransfection. $n = 4$ independent transfections. (B) Transfection rates in naive cells are also enhanced by the poly(U/UC) deletion and NS5A C2274R mutation. Naive Huh7.5 cells were transfected with WT and mutant Jc1/$^{NS5AB\text{-}mKO2\text{-}Bsd}$ transcripts and transfection rates (% mKO2$^+$) were assessed by flow cytometry 2 days later. $n = 4$ independent transfections. (C) Superinfection rates are also enhanced by the poly(U/UC) deletion and NS5A C2274R mutation. Jc1/ΔE1E2$^{NS5A\text{-}GFP}$ polyclonal replicon cells were infected with WT and mutant Jc1/$^{NS5AB\text{-}mKO2\text{-}Bsd}$ viral supernatants (normalized to the amount of HCV core per infection). Superinfection rates were assessed by flow cytometry 3 days later. $n = 3$ independent viral preparations and infections; error bars indicate the SEM.

The Jc1/$^{NS5AB\text{-}mKO2\text{-}Bsd}$ viral genomes were highly infectious and produced bright orange fluorescence in infected cells, permitting simple analysis of the dynamics of HCV superinfection in replicon-containing cells. These two characteristics allowed us, in the space of a few weeks, to select for a strain of HCV that could superinfect genotype 2a replicon-containing cells. Notably, the superinfectious HCV strain had two key characteristics: it displayed higher infectivity overall, even in naive cells, and it excluded the primary replicon in the space of 9 to 15 days.

Interestingly, the superinfectious phenotype was weaker in genotype 1b replicon-containing cells. This was not explained by higher levels of replication of the Con1 replicon; previous studies have demonstrated that Con1 is far less efficient at establishing replication than JFH-1-based replicons, but the steady-state RNA levels are equivalent (43, 44). Our results agree in both respects. The Con1 SGR/$^{NS5A\text{-}GFP}$ was >2-log less efficient at establishing replication compared to Jc1/ΔE1E2$^{NS5A\text{-}GFP\text{-}Bsd}$, but the RNA levels in GFP$^+$ cells were equivalent between replicons (data not shown). Therefore, the lower superinfection rates of adapted Jc1 in Con1 SGR/$^{NS5A\text{-}GFP}$ replicon cells may be due to differences in the construction of the replicons. Con1 SGR/$^{NS5A\text{-}GFP}$ is a bicistronic replicon with a neomycin selection cassette, containing only NS3-NS5B. Jc1/ΔE1E2$^{NS5A\text{-}GFP\text{-}Bsd}$, on the other hand, is monocistronic with a blasticidin selection cassette, also expressing core, truncated E1E2, p7, and NS2. These differences could modify the intracellular environment in a way that affects superinfection exclusion. Alternatively, and more provocatively, the adapted Jc1 may have been selected to specifically superinfect cells according to the genotype of the primary strain.

The importance of a blockade to viral entry in the process of superinfection exclusion has been controversial, since initial studies found no defect in entry of HIV particles pseudotyped with an HCV envelope (5). However, both increased and decreased expression of viral entry receptors can occur upon HCV infection, potentially enhancing or blockading HCV entry into infected cells (6, 45–48). Regardless of any effects on viral receptors, when a secondary replicon is "supertransfected" into cells already containing an HCV replicon, it replicates very poorly, clearly showing that postentry superinfection exclusion exists (7, 34). This postentry replication block may directly result from blocking replication of secondary viral RNA, or indirectly, by preventing translation of secondary viral RNA.

Initial analysis of the adaptive mutations acquired in the superinfectious strain suggested that the E1 A335S, p7 V756A, and NS5A C2274R mutations contributed significantly to the phenotype. Viral competition experiments using Jc1/$^{NS5AB\text{-}Barcode}$ strains demonstrated the importance of the p7 V756A and NS5A C2274R mutations and the poly(U/UC) deletion. However, mutations in E1, E2, or p7 are unlikely to allow the virus to overcome postentry superinfection exclusion, since these proteins only affect viral entry or assembly. The contribution of the E1 and p7 mutations to the superinfectious phenotype is likely a result of simply enhancing viral assembly and fusion, and increasing the number of secondary viral genomes in previously infected cells. Indeed, by "supertransfecting" viral transcripts into replicon-containing cells, thus focusing specifically on the postentry superinfection block, we found the NS5A C2274R mutation and poly(U/UC) deletions to be most crucial in overcoming the postentry block. Notably, when competition studies were carried out, an adapted Jc1 strain lacking the poly(U/UC) deletion established high levels of initial

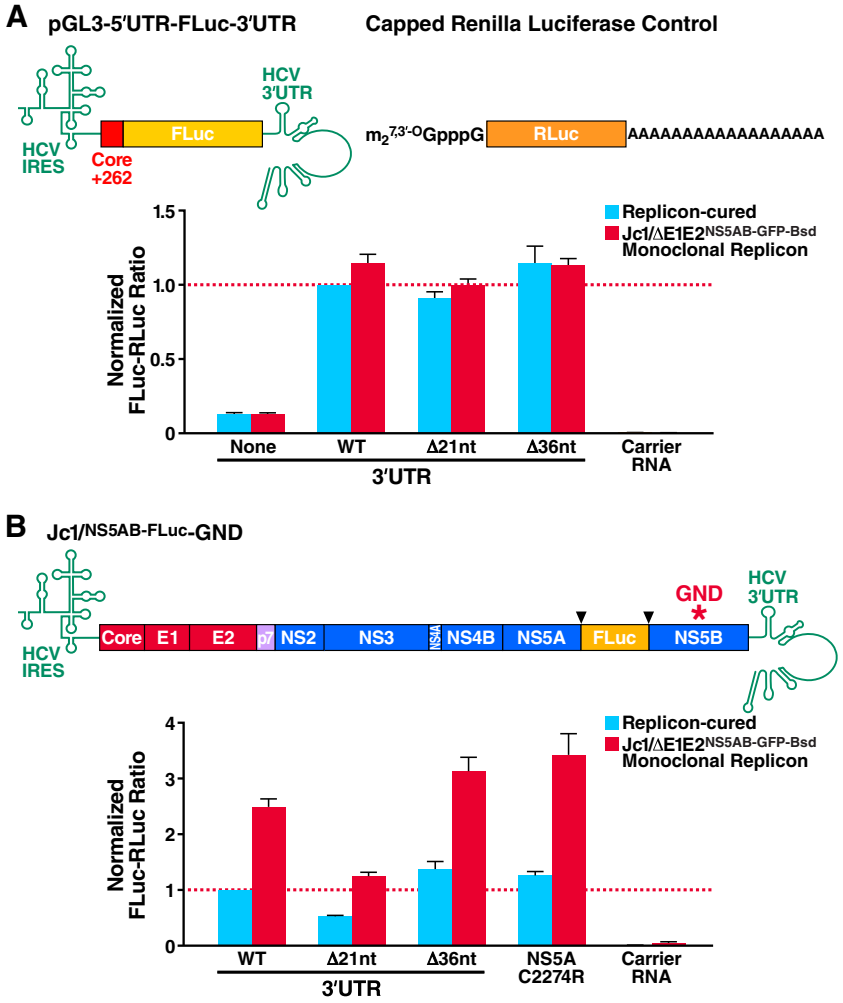

FIG 10 Viral RNA translation is not enhanced by the NS5A C2274R and Δ 3′UTR mutations. (A) Deletions of the poly(U/UC) tract do not enhance HCV IRES-mediated translation. Jc1/ΔE1E2$^{NS5A\text{-}GFP}$ polyclonal replicon cells and IFN-α replicon-cured cells were transfected with HCV IRES-dependent firefly luciferase (FLuc) transcripts containing WT and mutant HCV 3′UTRs, as well as a capped *Renilla* luciferase (RLuc) transcript as a transfection control. Core+262 refers to a fusion of 262 nt of HC-J6 core sequence to FLuc to enhance HCV IRES-mediated translation. The luciferase activity was assessed at 2 h posttransfection, and the ratio of FLuc/RLuc activity was normalized to the WT 3′UTR construct in replicon-cured cells. $n = 3$ independent transfections. (B) Histogram of normalized FLuc/RLuc ratios showing that NS5A C2274R and Δ 3′UTR mutations do not enhance translation of replication-incompetent viral RNAs. Cells were transfected as in panel A with Jc1/$^{NS5AB\text{-}FLuc}$-GND transcripts (polymerase defective, NS5B GDD→GND mutation) containing NS5A C2274R or Δ 3′UTR mutations. Arrowheads indicate NS5A/5B protease cleavage sites. $n = 3$ independent transfections of two replicates each; error bars indicate the SEM.

infection (day 3; Fig. 7B and C) but was excluded from the culture after viral spread and superinfection occurred (day 18). In conjunction with the "supertransfection" studies, the poly(U/UC) deletion appears quite important in allowing HCV to establish RNA replication in infected or replicon-containing cells.

Interestingly, neither the NS5A C2274R mutation nor the poly(U/UC) deletions affected viral RNA translation. It has previously been shown, using small FLuc reporter RNAs equivalent to those used in Fig. 10A, that HCV IRES-mediated translation is enhanced *in vivo* by 49- to 138-nt poly(U/UC) tracts independent of length (49). Our results agree with this finding and further demonstrate that deletions of the poly(U/UC) tract do not affect HCV IRES-mediated translation in full-length viral RNAs and in the context of a separate replicon. Further, we found that translation of full-length HCV transcripts, but not short reporter RNAs, was enhanced in replicon-containing cells. This agrees with previous findings that HCV IRES-mediated translation is enhanced in replicon-containing cells (37) but disagrees with results indicating that translation of a secondary subgenomic viral RNA is decreased in replicon-containing cells (5). However, Schaller et al. used a bicistronic construct in which translation of luciferase was driven by the HCV IRES and the viral polyprotein by EMCV IRES. In our study, all translation was driven by the native HCV IRES, which may be more reflective of natural HCV translation. Presumably, NS5A C2774R and the poly(U/UC) deletions allow HCV to overcome the postentry superinfection block by modulating HCV RNA replication.

Of note, superinfectious viruses also rapidly excluded the primary replicon or virus after superinfection (Fig. 7, Fig. 5). This phenomenon would act to further prevent co-occupancy of the same cell with multiple viral genomes and thus interstrain recombination. The mechanism by which the superinfectious virus excludes the primary replicon is unclear. We recently described a mechanism of intracellular competition between HCV strains

whereby mitosis of host cells leads to a genetic bottleneck in HCV diversity (17). The higher replicative capacity of the superinfectious strain may induce a bias in this intracellular competition in dividing cells, leading to eventual exclusion of the primary virus.

A number of prior studies focusing on the culture adaptation of JFH-1 and JFH-1-based chimeric strains identified the same adaptive mutations found in the present study. These mutations include, for example, p7 V756A (21), NS5A C2274R (50–52), and a shorter poly(U/UC) (35, 36). The typical approach to cell culture adaptation in HCV is to infect cells in long-term cultures, with intermittent serial passages of viral supernatants. It is likely that these culture conditions are also selecting for superinfectivity; our results indicate that superinfectious HCV strains exclude non-adapted strains and quickly dominate a culture. Thus, superinfectivity appears to correlate highly with overall viral fitness. Selection for superinfectivity in a natural patient setting, and possible exclusion of the primary strain, remains to be established. Transplantation of HCV-infected liver grafts into infected patients suggests that exclusion of the donor or recipient strain happens within as little as 1 day (53). It may be interesting in the future to infect mice with humanized livers with WT Jc1 and superinfect with Jc1 Mut7 to determine whether superinfection and viral dominance also occurs *in vivo*.

The postentry block to HCV superinfection has been postulated to result from sequestration of a limiting host factor(s) by the primary virus (6), as evidenced by a plateau in HCV RNA and protein levels shortly after infection. We found that the NS5A C2274R and poly(U/UC) deletion are key players in allowing a secondary virus to overcome the postentry superinfection block. In future studies, it will be interesting to determine whether the variants of these HCV proteins and RNA have a greater affinity for certain host proteins. Such host proteins would likely serve as rate-limiting factors in the HCV life cycle and, as such, would be excellent targets for antiviral therapies.

ACKNOWLEDGMENTS

We thank Ralf Bartenschlager (University of Heidelberg) for the Jc1 construct, Charles Rice (Rockefeller University) for Huh7.5 cells, Takaji Wakita (National Institute of Infectious Disease, Japan) for the JFH1 construct, Jing-hsiung Ou (University of Southern California) for pUC Con1, and Matthew Spindler (The J. David Gladstone Institutes) for the pSicoR construct. We are grateful to Marielle Cavrois and the Gladstone Flow Cytometry Core for assistance with flow cytometric assays. We thank John Carroll for help in preparation of the figures, and members of the Greene laboratory for helpful discussion and support.

This study was supported by the Gladstone Institutes and funds from the U.S. Public Health Service (T32 A1060537-05 [UCSF Program in Microbial Pathogenesis and Host Defense]) and the National Institutes of Health (R56 AI085056).

REFERENCES

1. **Michel N, Allespach I, Venzke S, Fackler OT, Keppler OT.** 2005. The Nef protein of human immunodeficiency virus establishes superinfection immunity by a dual strategy to downregulate cell surface CCR5 and CD4. Curr. Biol. **15:**714–723.
2. **Adams RH, Brown DT.** 1985. BHK cells expressing Sindbis virus-induced homologous interference allow the translation of nonstructural genes of superinfecting virus. J. Virol. **54:**351–357.
3. **Walters KA, Joyce MA, Addison WR, Fischer KP, Tyrrell DL.** 2004. Superinfection exclusion in duck hepatitis B virus infection is mediated by the large surface antigen. J. Virol. **78:**7925–7937.
4. **Folimonova SY.** 2012. Superinfection exclusion is an active virus-controlled function that requires a specific viral protein. J. Virol. **86:**5554–5561.
5. **Schaller T, Appel N, Koutsoudakis G, Kallis S, Lohmann V, Pietschmann T, Bartenschlager R.** 2007. Analysis of hepatitis C virus superinfection exclusion by using novel fluorochrome gene-tagged viral genomes. J. Virol. **81:**4591–4603.
6. **Tscherne DM, Evans MJ, von Hahn T, Jones CT, Stamataki Z, McKeating JA, Lindenbach BD, Rice CM.** 2007. Superinfection exclusion in cells infected with hepatitis C virus. J. Virol. **81:**3693–3703.
7. **Evans MJ, Rice CM, Goff SP.** 2004. Genetic interactions between hepatitis C virus replicons. J. Virol. **78:**12085–12089.
8. **Lee YM, Tscherne DM, Yun SI, Frolov I, Rice CM.** 2005. Dual mechanisms of pestiviral superinfection exclusion at entry and RNA replication. J. Virol. **79:**3231–3242.
9. **Pietschmann T, Kaul A, Koutsoudakis G, Shavinskaya A, Kallis S, Steinmann E, Abid K, Negro F, Dreux M, Cosset FL, Bartenschlager R.** 2006. Construction and characterization of infectious intragenotypic and intergenotypic hepatitis C virus chimeras. Proc. Natl. Acad. Sci. U. S. A. **103:**7408–7413.
10. **Dorner M, Horwitz JA, Donovan BM, Labitt RN, Budell WC, Friling T, Vogt A, Catanese MT, Satoh T, Kawai T, Akira S, Law M, Rice CM, Ploss A.** 2013. Completion of the entire hepatitis C virus life cycle in genetically humanized mice. Nature **501:**237–241.
11. **Horwitz JA, Dorner M, Friling T, Donovan BM, Vogt A, Loureiro J, Oh T, Rice CM, Ploss A.** 2013. Expression of heterologous proteins flanked by NS3-4A cleavage sites within the hepatitis C virus polyprotein. Virology **439:**23–33.
12. **Vogt A, Scull MA, Friling T, Horwitz JA, Donovan BM, Dorner M, Gerold G, Labitt RN, Rice CM, Ploss A.** 2013. Recapitulation of the hepatitis C virus life-cycle in engineered murine cell lines. Virology **444:**1–11.
13. **Blight KJ, McKeating JA, Rice CM.** 2002. Highly permissive cell lines for subgenomic and genomic hepatitis C virus RNA replication. J. Virol. **76:**13001–13014.
14. **Naldini L, Blomer U, Gallay P, Ory D, Mulligan R, Gage FH, Verma IM, Trono D.** 1996. In vivo gene delivery and stable transduction of nondividing cells by a lentiviral vector. Science **272:**263–267.
15. **Wakita T, Pietschmann T, Kato T, Date T, Miyamoto M, Zhao Z, Murthy K, Habermann A, Krausslich HG, Mizokami M, Bartenschlager R, Liang TJ.** 2005. Production of infectious hepatitis C virus in tissue culture from a cloned viral genome. Nat. Med. **11:**791–796.
16. **Kato T, Date T, Murayama A, Morikawa K, Akazawa D, Wakita T.** 2006. Cell culture and infection system for hepatitis C virus. Nat. Protoc. **1:**2334–2339.
17. **Webster B, Wissing S, Herker E, Ott M, Greene WC.** 2013. Rapid intracellular competition between hepatitis C viral genomes as a result of mitosis. J. Virol. **87:**581–596.
18. **Boson B, Granio O, Bartenschlager R, Cosset FL.** 2011. A concerted action of hepatitis C virus p7 and nonstructural protein 2 regulates core localization at the endoplasmic reticulum and virus assembly. PLoS Pathog. **7:**e1002144. doi:10.1371/journal.ppat.1002144.
19. **Zhong J, Gastaminza P, Cheng G, Kapadia S, Kato T, Burton DR, Wieland SF, Uprichard SL, Wakita T, Chisari FV.** 2005. Robust hepatitis C virus infection in vitro. Proc. Natl. Acad. Sci. U. S. A. **102:**9294–9299.
20. **Koutsoudakis G, Kaul A, Steinmann E, Kallis S, Lohmann V, Pietschmann T, Bartenschlager R.** 2006. Characterization of the early steps of hepatitis C virus infection by using luciferase reporter viruses. J. Virol. **80:**5308–5320.
21. **Gottwein JM, Jensen TB, Mathiesen CK, Meuleman P, Serre SB, Lademann JB, Ghanem L, Scheel TK, Leroux-Roels G, Bukh J.** 2011. Development and application of hepatitis C reporter viruses with genotype 1 to 7 core-nonstructural protein 2 (NS2) expressing fluorescent proteins or luciferase in modified JFH1 NS5A. J. Virol. **85:**8913–8928.
22. **Jones CT, Murray CL, Eastman DK, Tassello J, Rice CM.** 2007. Hepatitis C virus p7 and NS2 proteins are essential for production of infectious virus. J. Virol. **81:**8374–8383.
23. **Murray CL.** 2007. Genetic and biochemical analyses of the flaviviridae capsid proteins. Ph.D. thesis. Rockefeller University, New York, NY.
24. **Timpe JM, Stamataki Z, Jennings A, Hu K, Farquhar MJ, Harris HJ, Schwarz A, Desombere I, Roels GL, Balfe P, McKeating JA.** 2008. Hepatitis C virus cell-cell transmission in hepatoma cells in the presence of neutralizing antibodies. Hepatology **47:**17–24.
25. **Hazari S, Chandra PK, Poat B, Datta S, Garry RF, Foster TP, Kousoulas**

G, Wakita T, Dash S. 2010. Impaired antiviral activity of interferon alpha against hepatitis C virus 2a in Huh-7 cells with a defective Jak-Stat pathway. Virol. J. **7:**36.
26. **Cheng G, Chan K, Yang H, Corsa A, Pokrovskii M, Paulson M, Bahador G, Zhong W, Wt Delaney.** 2011. Selection of clinically relevant protease inhibitor-resistant viruses using the genotype 2a hepatitis C virus infection system. Antimicrob. Agents Chemother. **55:**2197–2205.
27. **Fournier C, Helle F, Descamps V, Morel V, Francois C, Dedeurwaerder S, Wychowski C, Duverlie G, Castelain S.** 2013. Natural selection of adaptive mutations in nonstructural genes increases trans-encapsidation of hepatitis C virus replicons lacking envelope protein genes. J. Gen. Virol. **94:**996–1008.
28. **Kolykhalov AA, Agapov EV, Rice CM.** 1994. Specificity of the hepatitis C virus NS3 serine protease: effects of substitutions at the 3/4A, 4A/4B, 4B/5A, and 5A/5B cleavage sites on polyprotein processing. J. Virol. **68:**7525–7533.
29. **Choi J, Lee KJ, Zheng Y, Yamaga AK, Lai MM, Ou JH.** 2004. Reactive oxygen species suppress hepatitis C virus RNA replication in human hepatoma cells. Hepatology **39:**81–89.
30. **Garcia-Rivera JA, Lin K, Hopkins S, Gregory MA, Wilkinson B, Gallay PA.** 2012. Development of a flow cytometry live cell assay for the screening of inhibitors of hepatitis C virus (HCV) replication. Open Virol. J. **6:**97–102.
31. **Lauring AS, Andino R.** 2011. Exploring the fitness landscape of an RNA virus by using a universal barcode microarray. J. Virol. **85:**3780–3791.
32. **White MJ, Fristensky BW, Thompson WF.** 1991. Concatemer chain reaction: a *Taq* DNA polymerase-mediated mechanism for generating long tandemly repetitive DNA sequences. Anal. Biochem. **199:**184–190.
33. **Witteveldt J, Evans MJ, Bitzegeio J, Koutsoudakis G, Owsianka AM, Angus AG, Keck ZY, Foung SK, Pietschmann T, Rice CM, Patel AH.** 2009. CD81 is dispensable for hepatitis C virus cell-to-cell transmission in hepatoma cells. J. Gen. Virol. **90:**48–58.
34. **Lohmann V, Hoffmann S, Herian U, Penin F, Bartenschlager R.** 2003. Viral and cellular determinants of hepatitis C virus RNA replication in cell culture. J. Virol. **77:**3007–3019.
35. **Li YP, Ramirez S, Gottwein JM, Scheel TK, Mikkelsen L, Purcell RH, Bukh J.** 2012. Robust full-length hepatitis C virus genotype 2a and 2b infectious cultures using mutations identified by a systematic approach applicable to patient strains. Proc. Natl. Acad. Sci. U. S. A. **109:**E1101–E1110.
36. **Murayama A, Weng L, Date T, Akazawa D, Tian X, Suzuki T, Kato T, Tanaka Y, Mizokami M, Wakita T, Toyoda T.** 2010. RNA polymerase activity and specific RNA structure are required for efficient HCV replication in cultured cells. PLoS Pathog. **6:**e1000885. doi:10.1371/journal.ppat.1000885.
37. **Tardif KD, Mori K, Siddiqui A.** 2002. Hepatitis C virus subgenomic replicons induce endoplasmic reticulum stress activating an intracellular signaling pathway. J. Virol. **76:**7453–7459.
38. **Krieger N, Lohmann V, Bartenschlager R.** 2001. Enhancement of hepatitis C virus RNA replication by cell culture-adaptive mutations. J. Virol. **75:**4614–4624.
39. **Han TX, Xu XY, Zhang MJ, Peng X, Du LL.** 2010. Global fitness profiling of fission yeast deletion strains by barcode sequencing. Genome Biol. **11:**R60.
40. **Smith AM, Heisler LE, Mellor J, Kaper F, Thompson MJ, Chee M, Roth FP, Giaever G, Nislow C.** 2009. Quantitative phenotyping via deep barcode sequencing. Genome Res. **19:**1836–1842.
41. **Tuteja R, Tuteja N.** 2004. Serial analysis of gene expression (SAGE): unraveling the bioinformatics tools. Bioessays **26:**916–922.
42. **Smith AM, Durbic T, Oh J, Urbanus M, Proctor M, Heisler LE, Giaever G, Nislow C.** 2011. Competitive genomic screens of barcoded yeast libraries. J. Vis. Exp. **54:**pii=2864. doi:10.3791/2864.
43. **Miyamoto M, Kato T, Date T, Mizokami M, Wakita T.** 2006. Comparison between subgenomic replicons of hepatitis C virus genotypes 2a (JFH-1) and 1b (Con1 NK5.1). Intervirology **49:**37–43.
44. **Binder M, Quinkert D, Bochkarova O, Klein R, Kezmic N, Bartenschlager R, Lohmann V.** 2007. Identification of determinants involved in initiation of hepatitis C virus RNA synthesis by using intergenotypic replicase chimeras. J. Virol. **81:**5270–5283.
45. **Liu S, Yang W, Shen L, Turner JR, Coyne CB, Wang T.** 2009. Tight junction proteins claudin-1 and occludin control hepatitis C virus entry and are downregulated during infection to prevent superinfection. J. Virol. **83:**2011–2014.
46. **Nakamuta M, Fujino T, Yada R, Aoyagi Y, Yasutake K, Kohjima M, Fukuizumi K, Yoshimoto T, Harada N, Yada M, Kato M, Kotoh K, Taketomi A, Maehara Y, Nakashima M, Enjoji M.** 2011. Expression profiles of genes associated with viral entry in HCV-infected human liver. J. Med. Virol. **83:**921–927.
47. **Reynolds GM, Harris HJ, Jennings A, Hu K, Grove J, Lalor PF, Adams DH, Balfe P, Hubscher SG, McKeating JA.** 2008. Hepatitis C virus receptor expression in normal and diseased liver tissue. Hepatology **47:**418–427.
48. **Sainz B, Jr, Barretto N, Martin DN, Hiraga N, Imamura M, Hussain S, Marsh KA, Yu X, Chayama K, Alrefai WA, Uprichard SL.** 2012. Identification of the Niemann-Pick C1-like 1 cholesterol absorption receptor as a new hepatitis C virus entry factor. Nat. Med. **18:**281–285.
49. **Wang H, Shen XT, Ye R, Lan SY, Xiang L, Yuan ZH.** 2005. Roles of the polypyrimidine tract and 3′ noncoding region of hepatitis C virus RNA in the internal ribosome entry site-mediated translation. Arch. Virol. **150:**1085–1099.
50. **Scheel TK, Gottwein JM, Jensen TB, Prentoe JC, Hoegh AM, Alter HJ, Eugen-Olsen J, Bukh J.** 2008. Development of JFH1-based cell culture systems for hepatitis C virus genotype 4a and evidence for cross-genotype neutralization. Proc. Natl. Acad. Sci. U. S. A. **105:**997–1002.
51. **Gottwein JM, Scheel TK, Jensen TB, Lademann JB, Prentoe JC, Knudsen ML, Hoegh AM, Bukh J.** 2009. Development and characterization of hepatitis C virus genotype 1-7 cell culture systems: role of CD81 and scavenger receptor class B type I and effect of antiviral drugs. Hepatology **49:**364–377.
52. **Liu S, Xiao L, Nelson C, Hagedorn CH.** 2012. A cell culture adapted HCV JFH1 variant that increases virus titers and permits the production of high titer infectious chimeric reporter viruses. PLoS One **7:**e44965. doi:10.1371/journal.pone.0044965.
53. **Ramirez S, Perez-del-Pulgar S, Carrion JA, Coto-Llerena M, Mensa L, Dragun J, Garcia-Valdecasas JC, Navasa M, Forns X.** 2010. Hepatitis C virus superinfection of liver grafts: a detailed analysis of early exclusion of non-dominant virus strains. J. Gen. Virol. **91:**1183–1188.